Translating GWAS-identified loci for cardiac rhythm and rate using an *in vivo*, image-based, large-scale genetic screen in zebrafish

Authors: Benedikt von der Heyde[1,2], Anastasia Emmanouilidou[1,2], Tiffany Klingström[1,2], Eugenia Mazzaferro[1,2], Silvia Vicenzi[1,2], Sitaf Jumaa[1,2], Olga Dethlefsen[3,4], Harold Snieder[5], Eco de Geus[6], Erik Ingelsson[2,7,8,9], Amin Allalou[2,10], Hannah L. Brooke[11], Marcel den Hoed[1,2]*

Affiliations:

[1]Department of Immunology, Genetics and Pathology, Uppsala University, Uppsala, Sweden.

[2]Science for Life Laboratory, Uppsala University, Uppsala, Sweden.

[3]Science for Life Laboratory, Uppsala University, Uppsala, Sweden.

[4]National Bioinformatics Infrastructure Sweden, Stockholm University, Stockholm, Sweden.

[5]Department of Epidemiology, University of Groningen, University Medical Center Groningen, Groningen, the Netherlands.

[6]Department of Biological Psychology, Vrije Universiteit Amsterdam, Amsterdam, the Netherlands.

[7]Department of Medical Sciences, Molecular Epidemiology, Uppsala University, Uppsala, Sweden.

[8]Department of Medicine, Division of Cardiovascular Medicine, Stanford University School of Medicine, Stanford, CA, USA.

[9]Stanford Cardiovascular Institute, Stanford University, Stanford, CA 94305.

[10]Department of Information Technology, Visual Information and Interaction, Uppsala University, Uppsala, Sweden.

[11]Department of Public Health and Caring Sciences, Uppsala University, Uppsala, Sweden.

*To whom correspondence should be addressed: marcel.den_hoed@igp.uu.se.

Abstract: Large-scale experimental follow-up studies of genetic loci identified by genome-wide association studies (GWAS) to identify causal genes remain rare. A meta-analysis of GWAS recently identified eight loci that are associated with heart rate variability (HRV) in data from 53,174 individuals. However, functional follow-up experiments – aiming to identify and characterize causal genes in these loci - have not yet been performed. We developed an image- and CRISPR-Cas9-based pipeline to systematically characterize candidate genes for HRV and heart rate in live zebrafish embryos and larvae. Nine zebrafish orthologues of six human candidate genes were targeted simultaneously in fertilized eggs from fish that transgenically express GFP on smooth muscle cells (Tg(*acta2*:GFP)) to visualize the beating heart. An automated analysis of 30s recordings of 384 live zebrafish atria at 2 and 5 days post-fertilization identified genes that influence HRV (*kiaa1755* and *gngt1*); heart rate (*kiaa1755*); sinoatrial conduction (*syt10*, *hcn4* and *kiaa1755*); and early cardiac development (*gngt1, neo1*). Besides identifying likely causal genes for cardiac rhythm and rate, we show that our pipeline is suitable for comprehensive, *in vivo*, image-based characterization of candidate genes using zebrafish embryos and larvae.

Introduction

Heart rate variability (HRV) reflects the inter-beat variation of heart rate. HRV is controlled by the sinoatrial node, which receives input from the autonomic nervous system. Autonomic imbalance, which has been associated with work stress and other modifiable or non-modifiable risk factors (*1*), is reflected in lower HRV. Lower HRV has been associated with higher cardiac morbidity and mortality (*2*), and with a higher risk of all-cause mortality (*3*). HRV can be quantified non-invasively using the RR interval of a 12-lead ECG, making HRV a useful clinical marker for perturbations of the autonomic nervous system. However, the genetic basis of HRV remains largely elusive.

Recently, we and others identified the first loci that are robustly associated with HRV, using a meta-analysis of genome-wide association studies (GWAS) with data from 53,174 participants (*4*). Eleven of the 17 associated single nucleotide polymorphisms (SNPs) overlapped with loci that we previously identified as being associated with resting heart rate (*5*), itself a risk correlate for cardiovascular mortality (*6, 7*). *In silico* functional annotation of the five loci that are associated with both HRV (*4*) and heart rate (*5*) previously resulted in the prioritisation of six candidate genes that are anticipated to be causal (*4*). Functional follow-up experiments - ideally *in vivo* - are required to conclude if these genes are indeed causal, and whether they influence HRV, heart rate, or even cardiac conduction.

Mouse models are commonly used in cardiac research, but mice show substantial differences in cardiac rate and electrophysiology compared with humans (*8*). Inherently, these differences complicate extrapolation of results from mouse models to humans (*8*). Additionally, rodents are not suitable for high-throughput *in vivo* screens of cardiac rhythm and rate. Such screens are essential to systematically characterize positional candidate genes in the large number of loci that have now been identified by GWAS for cardiac rhythm, rate (*9*) and conduction (*10*). Hence, novel model systems that facilitate systematic, *in vivo* characterization of a large number of candidate genes are desirable.

In recent years, the zebrafish has become an important model system for genetic and drug screens for human disease (*11, 12*). Amongst the many advantages of zebrafish larvae as a model system are their short generation time, large number of offspring produced regularly, relatively low maintenance costs, rapid early development, and optical transparency. Zebrafish have a fully functional, beating heart around 24 hours post-fertilization, and the ECG of the two-chambered zebrafish heart is comparable to that of humans (*13*). Fluorescently labeled transgenes facilitate visualization of cell types or tissues of interest, which can now be performed in high-throughput thanks to advances in automated positioning of non-embedded, live zebrafish embryos (*14*). In addition, the zebrafish has a well-annotated genome, with orthologues of at least 71.4% of human genes (*15*). These genes can now be targeted efficiently and in a multiplexed manner (i.e. multiple genes simultaneously) thanks to recent advances in Clustered, Regulatory Interspaced, Short Palindromic Repeats (CRISPR) and CRISPR-associated systems (Cas) (*16*). All characteristics combined

make zebrafish embryos an attractive model system to systematically characterize candidate genes for cardiac rhythm, rate and conduction.

The aim of this study was to objectively characterize the most promising candidate genes in GWAS-identified loci for HRV for a role in cardiac rhythm and rate using a large-scale, image-based screen in zebrafish embryos and larvae.

Results

Experimental pipeline for genetic screens of cardiac outcomes in zebrafish embryos and larvae

Our experimental pipeline is outlined in Figure 1. Founder mutants (F_0) were generated in which all nine zebrafish orthologues of six human candidate genes were targeted using a multiplexed CRISPR-Cas9 approach (Table 1, table S1) (*16*). Generating the mutants in a background with transgenically expressed fluorescently labelled smooth muscle cells (Tg[*acta2*:*gfp*]) allowed us to visualize the beating atrium with minimal background noise. F_0 mutants were in-crossed, and the atria of 384 F_1 embryos were recorded for 30 s at 2 days post fertilization (dpf). In addition, we captured bright field images of the embryos to quantify body size. Of the 384 imaged embryos, 326 were imaged again at 5dpf (fig. S1), to capture genetic effects on cardiac outcomes and body size at two key stages of early cardiac development (*17*).

At 2dpf, some embryos showed sinoatrial pauses (n=39, 10.3%) **(**movie S1) and arrests (n=36, 9.5%) (movie S2); cardiac edema (n=15, 4.0%); or uncontrolled atrial contractions (n=1, 0.2%) (movie S3). At 5dpf, a subset of larvae displayed sinoatrial pauses (n=9, 2.7%); sinoatrial arrests (n=3, 0.9%); cardiac edema (n=14, 4.2%); uncontrolled atrial contractions (n=9, 2.7%); or an abnormal cardiac morphology and impaired cardiac contractility (n=6, 1.8%) (movie S4). In the 279 embryos without cardiac abnormalities that survived quality control at 2dpf (fig. S1), HRV was 15.5±10 ms (mean±SD) and heart rate 208±24 bpm. In the 291 larvae included in the analysis at 5dpf, HRV was 13.18±17.06 ms and heart rate 265±35 bpm (Table 2)**.**

After imaging at 5dpf, all larvae were sequenced at the nine CRISPR-Cas9 targeted sites (2x250 bp), and transcript-specific dosages were generated by weighting the number of mutated alleles by their predicted impact on protein function. A total of 164 unique mutations were identified across the nine CRISPR-targeted sites, ranging from three unique mutations in *hcn4l* to 37 in *kiaa1755_2* (table S2). Frameshift mutations were most common (48.8%), followed by missense variants (24.4%), in-frame deletions (24.6%), and synonymous variants (4.9%). Eighty-seven, sixty-nine and eight variants were predicted to have a high, moderate, and low impact on protein function, respectively. Mutant allele frequencies ranged from 4.1% for *hcn4l* to 92.0% for *neo1b* (table S3).

Genetic effects on HRV, heart rate, cardiac abnormalities and body size

We examined the effect of the induced mutations on HRV and heart rate after exclusion of cases with cardiac abnormalities like sinoatrial pauses or arrests, uncontrolled atrial contractions, edema, and abnormal morphology or contractility (primary analyses, fig. S1). We also examined the impact of mutations on cardiac abnormalities that occurred in at least five embryos (2dpf) or larvae (5dpf), as well as on body size (secondary analyses, fig. S1).

Each additional mutated allele in *gngt1* was associated with higher odds of abnormal cardiac morphology and impaired cardiac contractility at 2dpf (table S4), as

well as with higher odds of cardiac edema and a higher HRV at 5dpf (Fig. 2, table S5). *Gngt1* mutants also had a smaller dorsal body surface area at 5dpf.

Each additional mutated allele in *syt10* was associated with higher odds of a sinoatrial pause at 2dpf (table S4).

Each additional mutated allele in *hcn4* was associated with higher odds of sinoatrial pauses as well as with higher odds of sinoatrial arrests at 2dpf (table S4). In larvae free from severe cardiac abnormalities, each additional mutated allele in *hcn4* was associated with a trend for higher heart rate at 5dpf (Fig. 2, tables S5 and S6), without affecting body size (table S7). Mutations in *hcn4l* were positively associated with lateral body surface area at 5dpf (table S7), without affecting cardiac rhythm or rate at 2dpf or 5dpf.

Mutations in *neo1a* and *neo1b* did not affect heart rhythm, rate, or cardiac abnormalities at 2dpf. However, embryos with mutations in *neo1a* tended to be stockier - with a trend for shorter stature and with a larger dorsal body surface area normalized for length - while embryos with mutations in *neo1b* had a larger lateral body surface area at 2dpf. At 5dpf, mutations in *neo1a* were associated with lower odds of abnormal cardiac morphology and impaired cardiac contractility, uncontrolled atrial contractions (P=0.052), and edema (table S4), but not with body size.

Each additional mutated allele in the main transcript of *kiaa1755_1* was associated with a higher HRV and a trend for a higher heart rate at 2dpf (Fig. 2, tables S5 and S6). Mutations in *kiaa1755_1* were also associated with a larger body volume at 5dpf (table S7). Embryos with mutations in *kiaa1755_2* tended to be shorter and smaller at 2dpf (table S7), and had higher odds of sinoatrial pause and a higher heart rate at 5dpf (Fig. 2, tables S4-S6).

Five of the six human candidate genes taken forward for experimental follow-up showed at least one relevant cardiac phenotype in zebrafish embryos or larvae (i.e. *GNGT1*, *SYT10*, *HCN4*, *NEO1*, *KIAA1755*). Only a trend towards an effect - on sinoatrial pauses at 2dpf - was observed for *RGS6*. We next examined the druggability of the five genes for which we showed most evidence of a causal role using the drug-gene interaction (DGI) database. This only highlighted *HCN4* as druggable (*18*). Indeed, ivabradine is already being used as an open channel blocker of *HCN4* (19). We next identified interaction partners of the proteins encoded by the five genes using GeneMania (*20*) and STRING (*21*). A total of 49 interacting partners were identified, 31 of which were considered druggable by DGI, or belong to a “favorable” protein family. Seven of these are targeted by FDA-approved medication (table S8), amongst which are anti-hypertensive (e.g. Telmisartan, Iloprost and Diazoxide, among others) and neuromuscular blocking agents (i.e. Botulinum toxin type A).

Discussion

Large-scale, *in vivo* follow-up studies of candidate genes in GWAS-identified loci remain sparse. Here we present an objective, image-based pipeline to systematically characterize candidate genes for cardiac rhythm, rate, and development (Fig. 1). Using a zebrafish model system, we identified orthologues of genes in heart-rate variability-associated loci that influence not only heart rate variability (*kiaa1755*, *gngt1*) and heart rate (*kiaa1755*), but also cardiac development (*gngt1, neo1a*, *neo1b*), the odds of sinoatrial pauses and arrests (*hcn4, syt10, kiaa1755*) and body size (*kiaa1755, hcn4, gngt1, neo1a*, *neo1b*). These results add weight to the notion that the human equivalents of these genes are likely causal for cardiac rhythm and rate.

The HRV increasing allele (T) of rs4262 in the 5' untranslated region of *GNG11* is associated with a lower expression of *GNG11* in the tibial artery, atrial appendage and aorta (GTEx (*22*)). This is directionally consistent with 5dpf *gngt1* mutant zebrafish larvae - i.e. mutants for the zebrafish orthologue of the human paralogues *GNGT1* and *GNG11* (*23*) - having a higher HRV. *GNG11* encodes the γ-subunit of a G-protein complex, which interacts with G-protein-coupled inwardly rectifying potassium channels (GIRKs) that transduce signals rapidly enough to induce changes in HRV (*24*). The zebrafish heart normally has a tube-like appearance at 28 hours post fertilization (hpf) (*25*). A higher odds of abnormal cardiac morphology, contractility and edema with each additional mutated *gngt1* allele at 5 but not 2dpf suggests that this gene affects cardiac development between 2 and 5dpf.

SYT10 belongs to the synaptogamins: transmembrane proteins that are involved in regulation of membrane trafficking in neurons (*26*), which is important for neurotransmitter release (*27*). Variants in/near *SYT10* have previously been associated with HRV (*4*) as well as with heart rate (*5*). We observed an effect of mutations in *syt10* on the odds of sinoatrial pauses at 2dpf. Since *SYT10* is mainly expressed in brain, tibial nerve and pituitary (GTEx (*22*)), mutations in *syt10* may affect the odds of sinoatrial pauses through altered neurotransmitter release.

The locus harboring *HCN4* has been flagged in GWAS for HRV (*4*), heart rate (*5*) and atrial fibrillation (*28*). *HCN4* is arguably the most well-characterized gene in the context of cardiac rhythm. It belongs to the family of "funny" channels, aptly named for being activated upon hyperpolarization. It is expressed in the sinoatrial node (*29, 30*) and plays an important role in cardiac pace making (*31*). The heart-rate lowering agent ivabradine (*32*) is an open channel blocker of *HCN4*, and reduces cardiovascular and all-cause mortality in heart failure patients (*33*). Hcn4$^{-/-}$ mice die prenatally, and analyses of their hearts show no arrhythmias and a lower heart rate compared with wildtype and heterozygotes (*31*). In line with this, humans that are heterozygous for an *HCN4* loss of function mutation are typically characterized by bradycardia. We identified nine zebrafish embryos that were compound heterozygous for mutations in *hcn4*, and one embryo that was compound heterozygous for *hcn4l*, without a deviation from HWE for either gene (table S3). Four of the nine compound heterozygous larvae for *hcn4*, and six of the eight larvae that were heterozygous for

mutations in *hcn4* as well as *hcn4l* showed a sinoatrial arrest before or during the atrial recording at 2dpf. Zebrafish embryos can survive without a functional heart at this stage, thanks to tissue oxygenation by diffusion (*34*). This allowed us to witness genetically driven cardiac arrests, which would have been lethal in embryos of other species. At 5dpf, larvae carrying mutations in *hcn4* that were free from severe cardiac abnormalities tended to have a higher heart rate than larvae without CRISPR-induced mutations. This unexpected result may reflect overcompensation by *hcn4l*.

In addition to the locus in *HCN4*, the GWAS for HRV identified an independent locus in the adjacent *NEO1* (*4*). Neogenin-1 is a transmembrane receptor that is involved in cell migration, angiogenesis and neuronal survival (reviewed by Wilson et al. (*35*)). In line with our results, morpholino-mediated knockdown of *neo1a* expression in zebrafish larvae was previously shown to result in shorter, thicker larvae due to defects in somitogenesis, with loss of neuronal differentiation due to malformation of the neural tube (*36*). *NEO1* has a pro-apoptotic function in humans (*35*), so the cardioprotective effect we observed in 5dpf mutants may result from inefficient propagation of apoptotic signals by specific effectors. Inhibiting NEO1 in early development may thus help protect cardiac integrity - perhaps temporarily - but will likely have adverse effects due to inadequate apoptosis at later stages of development.

Non-synonymous SNPs in *KIAA1755* have been identified in GWAS for HRV (*4*) and heart rate (*5*). In humans, the C-allele of the HRV-associated rs6123471 in the 3' UTR of *KIAA1755* is associated with a lower expression of *KIAA1755* in brain and aorta (GTEx, (*22*)), a higher HRV (*4*), and a lower heart rate (*5*). Our results show that mutations in *kiaa1755_1* predispose to a higher HRV and, in a sensitivity analysis, a higher heart rate at 2dpf. Mutations in *kiaa1755_2* on the other hand result in a higher heart rate and higher odds of sinoatrial pauses at 5dpf. Hence, a higher HRV at 2dpf for each additional mutated allele in *kiaa1755_1* is directionally consistent with results in humans, while the effects of mutations in *kiaa1755_1* and *kiaa1755_2* on heart rate are not. We cannot exclude the possibility that the GWAS-identified association of the *KIAA1755* locus - and possibly other loci - with heart rate was driven by HRV. This would explain why the eleven HRV-associated loci that showed evidence of an association with heart rate all did so in the expected direction from a phenotypic point of view (i.e. opposite) (*4*). Genetic effects on HRV and heart rate were mutually adjusted in our study, which may have revealed the unbiased direction of effect for mutations in *KIAA1755* on heart rate. *KIAA1755* is a previously uncharacterized gene that shows a broad expression pattern, including different brain regions and the left atrial appendage (GTEx, (*22*)). Future mechanistic studies are required to distill how *KIAA1755* influences heart rhythm and rate.

Of the five genes for which we show causal effects, only *HCN4* is highlighted as being druggable by DGIdb. The protein encoded by *HCN4* has already been targeted using several compounds (*37*). Although four of the five causal genes are not highlighted as being druggable by current pharmaceutical standards, targeting via

antisense oligonucleotides or antibodies still remains a possibility that can be looked into further. Expanding our search revealed several druggable interaction partners of causal genes that are already targeted by FDA-approved anti-hypertensive and neuromuscular blocking agents, amongst others. For existing drugs that target interaction partners of the five causal genes, it is worthwhile examining their effect on cardiac rhythm, rate and development, since repurposing FDA-approved drugs would imply the quickest and safest route to the clinic.

A few limitations of our study should be discussed. Firstly, acquiring 30s recordings implies that false negatives for sinoatrial pauses or arrests are inevitable. In fact, we observed 54 pauses or arrests at 2dpf (14.3%) and eight at 5dpf (2.5%) while positioning the larva for imaging, without observing abnormalities during the 30s recording. This suggests that at least 15.9% of all embryos without a sinoatrial pause at 2dpf are false negatives, which negatively affects the statistical power to find genetic effects. This limitation will have resulted in conservative effect estimates. Secondly, CRISPR guide-RNAs with predicted off-targets free from mismatches were avoided. However, three of the selected targets - i.e. for *gngt1*, *hcn4* and *kiaa1755_2* - have intronic or exonic off-targets with three mismatches (table S1). Human orthologues of potential off-targets *dclk1* and *galnt10* have previously been associated with heart-rate variability-related traits (*38*) (*dclk1*), as well as with carotid intima-media thickness (*39*) and body mass index (*40-42*) (*galnt10*). Based on the number of mismatches in combination with predictions by Varshney *et al*., off-target effects are unlikely to have influenced our results (*43*). Thirdly, we propose to in-cross mosaic founder mutants (F_0) and phenotypically screen and sequence the F_1 generation. For some genes, this will yield inconclusive results due to a small number of screened larvae with 0 or 2 mutated alleles (e.g. *rgs6*), if all embryos are produced by a very small number of founder mutants, if the efficiency of the gRNA is higher or lower than expected, or if successfully targeting the gene influences viability, amongst others. On the other hand, screening the F_0 or F_2 generation both have their own advantages and disadvantages, and we would argue that when aiming to systematically characterize a large number of candidate genes, non-conclusive results for a small subset of candidate genes in the primary screen is not problematic. Fourthly, we recorded the atrium only, to enable a higher frame rate, a higher resolution in time, and a higher statistical power to detect small genetic effects on HRV. As a result, ventricular abnormalities that may have occurred were not registered, and uncontrolled atrial contractions may reflect atrial fibrillation, premature atrial contractions, high atrial rate, or atrial tachycardia. Additional studies with a larger frame and longer acquisition time are required to replicate and clarify the effect of mutations in *neo1a* on uncontrolled atrial contractions. Finally, our sample contained very few embryos with mutations in *hcn4l* and *rgs6*, and only a few embryos that were wildtype for *neo1b*. Both very low and very high mutagenic efficiencies have a negative effect on the statistical power to find true genetic effects. In spite of this limitation, we were able to detect significant effects of mutations in all

genes except *rgs6*, for which we observed a trend for an effect on the odds of sinoatrial pauses at 2dpf.

Our study benefits from a repeated measures design, which enabled us to capture genetic effects at different stages of early development in zebrafish. Furthermore, the high-throughput setup allowed us to examine the effect of multiple genes simultaneously, in an unprecedented sample size for *in vivo* genetic screens. Our results demonstrate that a large sample size is paramount to robustly detect genetic effects on complex traits in zebrafish embryos and larvae, even for functional knockout mutations. Identifying CRISPR-Cas9-induced mutations allele-specifically helped us classify larvae as heterozygous and compound heterozygous, which in turn helped pinpoint the true effect of mutations in these genes.

Our study is based on an objective, high-throughput imaging approach and aimed to identify and characterize causal genes in GWAS-identified loci for HRV. In all genes that show an effect on HRV (*kiaa1755* and *gngt1*), directions of effect were directionally consistent with eQTL associations (based on GTEx (*22*)). This emphasizes the merit of our model system and the robustness of our findings. Our results extend beyond the continuous outcomes of primary interest and also provide insights into genetic effects on clinical endpoints.

Materials and Methods

Study design

The aim of this study was to characterize candidate genes that influence HRV in an objective and high-throughput manner in zebrafish embryos and larvae. We generated multiplexed CRISPR-Cas9 mutants in a line with GFP-labelled α-smooth muscle cells Tg(*acta2:GFP*) to visualize the beating atrium. Founder mutants were in-crossed, and 384 offspring were phenotypically screened and sequenced. Since the mutant allele frequency varies across target sites, and since the effect size of null mutations on outcomes of interest varies across candidate genes, *a priori* power calculations could not be performed. We opted for n=384 to allow multiplexed sequencing in a single lane of a MiSeq. Imaging embryos and larvae requires anesthesia. Since anesthesia influences heart rate, we first established the minimal concentration of tricaine that is needed to anesthetize larvae at 2dpf and 5dpf. Before imaging, embryos and larvae were exposed to a standard concentration of tricaine (100 µg/ml) for a standard amount of time (1 min), to minimize variation. The acquired videos were automatically quantified using a custom-written MatLab script (see Supplementary Methods). The quality of every quantified signal was confirmed manually using a graphical representation of the results. The larvae were excluded from the genetic association analysis if one or more beats were missed in the automatic quantification.

Husbandry & microinjections

A zebrafish line with GFP-labelled α-smooth muscle cells Tg(*acta2*:GFP) (*44*) was used to visualize the beating heart. To this end, eggs from an in-cross of Tg(*acta2*:GFP) fish were co-injected with a mix of Cas9 mRNA (final concentration 150 ng/µl) and all nine gRNAs (final concentration 25 ng/µl each) in a total volume of 2nL at the single-cell stage. CRISPR-Cas9 injected embryos were optically screened for the presence of Tg(*acta2*:GFP) at 2 days post fertilization (dpf), using an automated fluorescence microscope (EVOS FL Cell imaging system, ThermoFisher Scientific, Waltham, USA). Tg(*acta2*:GFP) carriers were retained and raised to adulthood in systems with circulating, filtered and temperature controlled water (Aquaneering, Inc, San Diego, CA). All procedures and husbandry were conducted in accordance with Swedish and European regulations, and have been approved by the Uppsala University Ethical Committee for Animal Research (C142/13 and C14/16).

Experimental procedure HRV

The founder mutants (F_0 generation) were only used for reproduction. After crossing the founder mutants, F_1 embryos were used for experiments. Eggs were collected after F_0 fish were allowed to reproduce for 45 mins to minimize variation in developmental stage. Fertilized eggs were placed in an incubator at 28.5°C. At 1dpf, embryos were dechorionated using pronase (Roche Diagnostics, Mannheim, Germany).

At 2dpf, embryos were removed from the incubator and allowed to adapt to controlled room temperature (21.5 °C) for 20 mins. Individual embryos were exposed to 100 µg/ml Tricaine (MS-222, Sigma-Aldrich, Darmstadt, Germany) for 1 min before being aspirated, positioned in the field of view of a fluorescence microscope, and oriented dorsally using a Vertebrate Automated Screening Technology (VAST) BioImager (Union Biometrica Inc., Geel, Belgium). We subsequently acquired twelve whole-body images, one image every 30 degrees of rotation, using the camera of the VAST BioImager to quantify body length, dorsal and lateral surface area and volume, as well as the presence or absence of cardiac edema. The VAST BioImager then positioned and oriented the larva to visualize the beating atrium and triggered the upright Leica DM6000B fluorescence microscope to start imaging using a HCX APO L 40X/0.80 W objective and L5 ET, k filter system (Micromedic AB, Stockholm, Sweden). Images of the beating atrium were acquired for 30s at a frame rate of 152 frames/s using a DFC365 FX high-speed CCD camera (Micromedic AB, Stockholm, Sweden). After acquisition, the larvae were dispensed into a 96-well plate, rinsed from tricaine, and placed back into the incubator. The procedure was repeated at 5dpf (i.e. the larval stage), to allow genetic effects that influence HRV and heart rate differently at different stages of development to be captured (*17*). After imaging at 5dpf, the larvae were once again dispensed into 96-well plates, sacrificed, and stored at -80°C for further processing.

Quantification of cardiac traits and body size

A custom-written MATLAB script was used to convert the images acquired by the CCD camera into quantitative traits. To acquire the heart rate, each frame of the sequence was correlated with a template frame. The repeating pattern yields a periodic graph from the correlation values and by detecting the peaks in the graph we can assess the heart rate. The template frame should represent one of the extreme states in the cardiac cycle, i.e. end-systole or end-diastole. To detect these frames, we examined the correlation between the first 100 frames. The combination of frames that showed the lowest correlation corresponded to the heart being in opposite states. One of these frames was chosen as the template (*45*).

This numeric information was subsequently used to quantify: 1) heart rate as the inverse of RR-interval; 2) the standard deviation of the normal-to-normal RR interval (SDNN); and 3) the root mean square of successive heart beat interval differences (RMSSD). Finally, a graph of pixel changes over time was generated across the 30s recording to help annotate the script's performance. The files containing the inter-beat-intervals were used to objectively quantify sinoatrial pauses (i.e. the atrium stops beating for longer than 3x the median inter-beat-interval of the larva, movie S1) and sinoatrial arrests (i.e. the atrium stops beating for longer than 2s, movie S2) using a custom-written Stata script. The graphs of pixel changes over time were also used to identify larvae with other abnormalities in cardiac rhythm. Such abnormalities were annotated as: uncontrolled atrial contractions (movie S3); abnormal cardiac

morphology (i.e. a tube-like atrium, movie S4); or impaired cardiac contractility (i.e. a vibrating rather than a contracting atrium, movie S4). These phenotypes were annotated independently by two investigators (BvdH and MdH), resulting in an initial concordance rate >90%. Discrepancies in annotation were discussed and re-evaluated to reach consensus.

Bright-field images of the larvae were used to assess body length, dorsal and lateral surface area, and volume. Images were automatically segmented and quantified using a custom-written CellProfiler (*46*) pipeline, followed by manual annotation for segmentation quality. Larvae with suboptimal segmentation quality due to the presence of an air-bubble, a bent body, an incomplete rotation within the capillary, partial capturing of the larva, or an over-estimation of size were replaced by images with a 180° difference in rotation, or excluded if that image was also sub-optimally segmented. The larva was excluded from the analysis for body volume if more than four of the 12 images had a bad segmentation.

Statistical analysis

The standard deviation of NN-intervals (SDNN) and the root mean square of successive differences (RMSSD) were strongly correlated at 2dpf (r^2=0.77) and 5dpf (r^2=0.85), so a composite endpoint 'HRV' was calculated as the average of SDNN and RMSSD. In larvae free from sinoatrial pauses and arrests, abnormal cardiac morphology, impaired cardiac contractility, and edema HRV and heart rate at 2dpf (n=279) or 5dpf (n=291) were inverse-normally transformed to ensure a normal distribution, and to allow comparison of effect sizes across traits. Please see the supplementary methods for a detailed description of the cardiac phenotypes that were used as exclusion criteria for the analysis for HRV and heart rate. Genetic effects on HRV and heart rate were subsequently examined using hierarchical linear models at 2dpf and 5dpf separately (Stata's xtmixed), mutually adjusted for the other outcome (i.e. heart rate and HRV) and time of imaging (fixed factors), and with larvae nested in batches (random factor with fixed slope). Embryos and larvae in which a sinoatrial pause and/or arrest was observed in between positioning and recording were excluded from the analysis (see table S6 for a sensitivity analysis). In secondary analyses, genetic effects were examined for cardiac abnormalities that were observed in ≥5 larvae at 2dpf and/or 5dpf, using a logistic regression analysis. Genetic effects on body size were also examined, using hierarchical linear models on inverse-normally transformed outcomes.

For dichotomous as well as continuous outcomes, genetic effects were examined using an additive model, with dosage scores for all target sites as independent exposures in the same model, i.e. mutually adjusted for effects of mutations in the other orthologues. Missing genotypes were imputed at the mean in this analysis. For each outcome, association analyses were examined for the main transcript of the orthologue. All statistical analyses were performed using Stata MP 14.2.

Supplementary Materials

Materials and Methods

Fig. S1. Experimental flow chart.

Table S1. Overview of zebrafish orthologues and designed gRNAs.

Table S2. Unique variants and affected transcripts.

Table S3. Mutant allele frequencies.

Table S4. Transcript-specific association analysis for dichotomous cardiac outcomes.

Table S5. Transcript-specific association analysis for HRV and heart rate.

Table S6. Transcript-specific association analysis for heart rate variability and heart rate in larvae without a sinoatrial pause before or after the recording.

Table S7. Transcript-specific association analyses for body size.

Table S8. Druggability of interacting partners.

Movie S1. Sinoatrial pause.

Movie S2. Sinoatrial arrest.

Movie S3. Uncontrolled atrial contractions.

Movie S4. Abnormal morphology and reduced contractility.

References and Notes:

1. J. F. Thayer, S. S. Yamamoto, J. F. Brosschot, The relationship of autonomic imbalance, heart rate variability and cardiovascular disease risk factors. *Int. J. Cardiol.* **141**, 122-131 (2010).
2. M. C. de Bruyne, J. A. Kors, A. W. Hoes, P. Klootwijk, J. M. Dekker, A. Hofman, J. H. van Bemmel, D. E. Grobbee, Both decreased and increased heart rate variability on the standard 10-second electrocardiogram predict cardiac mortality in the elderly: the Rotterdam Study. *Am. J. Epidemiol.* **150**, 1282-1288 (1999).
3. J. M. Dekker, E. G. Schouten, P. Klootwijk, J. Pool, C. A. Swenne, D. Kromhout, Heart rate variability from short electrocardiographic recordings predicts mortality from all causes in middle-aged and elderly men - The zutphen study. *Am. J. Epidemiol.* **145**, 899-908 (1997).
4. I. M. Nolte, M. L. Munoz, V. Tragante, A. T. Amare, R. Jansen, A. Vaez, B. von der Heyde, C. L. Avery, J. C. Bis, B. Dierckx, J. van Dongen, S. M. Gogarten, P. Goyette, J. Hernesniemi, V. Huikari, S. J. Hwang, D. Jaju, K. F. Kerr, A. Kluttig, B. P. Krijthe, J. Kumar, S. W. van der Laan, L. P. Lyytikainen, A. X. Maihofer, A. Minassian, P. J. van der Most, M. Muller-Nurasyid, M. Nivard, E. Salvi, J. D. Stewart, J. F. Thayer, N. Verweij, A. Wong, D. Zabaneh, M. H. Zafarmand, A. Abdellaoui, S. Albarwani, C. Albert, A. Alonso, F. Ashar, J. Auvinen, T. Axelsson, D. G. Baker, P. I. W. de Bakker, M. Barcella, R. Bayoumi, R. J. Bieringa, D. Boomsma, G. Boucher, A. R. Britton, I. Christophersen, A. Dietrich, G. B. Ehret, P. T. Ellinor, M. Eskola, J. F. Felix, J. S. Floras, O. H. Franco, P. Friberg, M. G. J. Gademan, M. A. Geyer, V. Giedraitis, C. A. Hartman, D. Hemerich, A. Hofman, J. J. Hottenga, H. Huikuri, N. Hutri-Kahonen, X. Jouven, J. Junttila, M. Juonala, A. M. Kiviniemi, J. A. Kors, M. Kumari, T. Kuznetsova, C. C. Laurie, J. D. Lefrandt, Y. Li, Y. Li, D. Liao, M. C. Limacher, H. J. Lin, C. M. Lindgren, S. A. Lubitz, A. Mahajan, B. McKnight, H. M. Zu Schwabedissen, Y. Milaneschi, N. Mononen, A. P. Morris, M. A. Nalls, G. Navis, M. Neijts, K. Nikus, K. E. North, D. T. O'Connor, J. Ormel, S. Perz, A. Peters, B. M. Psaty, O. T. Raitakari, V. B. Risbrough, M. F. Sinner, D. Siscovick, J. H. Smit, N. L. Smith, E. Z. Soliman, N. Sotoodehnia, J. A. Staessen, P. K. Stein, A. M. Stilp, K. Stolarz-Skrzypek, K. Strauch, J. Sundstrom, C. A. Swenne, A. C. Syvanen, J. C. Tardif, K. D. Taylor, A. Teumer, T. A. Thornton, L. E. Tinker, A. G. Uitterlinden, J. van Setten, A. Voss, M. Waldenberger, K. C. Wilhelmsen, G. Willemsen, Q. Wong, Z. M. Zhang, A. B. Zonderman, D. Cusi, M. K. Evans, H. K. Greiser, P. van der Harst, M. Hassan, E. Ingelsson, M. R. Jarvelin, S. Kaab, M. Kahonen, M. Kivimaki, C. Kooperberg, D. Kuh, T. Lehtimaki, L. Lind, C. M. Nievergelt, C. J. O'Donnell, A. J. Oldehinkel, B. Penninx, A. P. Reiner, H. Riese, A. M. van Roon, J. D. Rioux, J. I. Rotter, T. Sofer, B. H. Stricker, H. Tiemeier, T. G. M. Vrijkotte, F. W. Asselbergs, B. Brundel, S. R. Heckbert, E. A. Whitsel, M. den Hoed, H. Snieder, E. J. C. de Geus, Genetic loci associated with heart rate variability and their effects on cardiac disease risk. *Nat Commun* **8**, 15805 (2017).
5. M. den Hoed, M. Eijgelsheim, T. Esko, B. J. Brundel, D. S. Peal, D. M. Evans, I. M. Nolte, A. V. Segre, H. Holm, R. E. Handsaker, H. J. Westra, T. Johnson, A. Isaacs, J. Yang, A. Lundby, J. H. Zhao, Y. J. Kim, M. J. Go, P. Almgren, M.

Bochud, G. Boucher, M. C. Cornelis, D. Gudbjartsson, D. Hadley, P. van der Harst, C. Hayward, M. den Heijer, W. Igl, A. U. Jackson, Z. Kutalik, J. Luan, J. P. Kemp, K. Kristiansson, C. Ladenvall, M. Lorentzon, M. E. Montasser, O. T. Njajou, P. F. O'Reilly, S. Padmanabhan, B. St Pourcain, T. Rankinen, P. Salo, T. Tanaka, N. J. Timpson, V. Vitart, L. Waite, W. Wheeler, W. Zhang, H. H. Draisma, M. F. Feitosa, K. F. Kerr, P. A. Lind, E. Mihailov, N. C. Onland-Moret, C. Song, M. N. Weedon, W. Xie, L. Yengo, D. Absher, C. M. Albert, A. Alonso, D. E. Arking, P. I. de Bakker, B. Balkau, C. Barlassina, P. Benaglio, J. C. Bis, N. Bouatia-Naji, S. Brage, S. J. Chanock, P. S. Chines, M. Chung, D. Darbar, C. Dina, M. Dorr, P. Elliott, S. B. Felix, K. Fischer, C. Fuchsberger, E. J. de Geus, P. Goyette, V. Gudnason, T. B. Harris, A. L. Hartikainen, A. S. Havulinna, S. R. Heckbert, A. A. Hicks, A. Hofman, S. Holewijn, F. Hoogstra-Berends, J. J. Hottenga, M. K. Jensen, A. Johansson, J. Junttila, S. Kaab, B. Kanon, S. Ketkar, K. T. Khaw, J. W. Knowles, A. S. Kooner, J. A. Kors, M. Kumari, L. Milani, P. Laiho, E. G. Lakatta, C. Langenberg, M. Leusink, Y. Liu, R. N. Luben, K. L. Lunetta, S. N. Lynch, M. R. Markus, P. Marques-Vidal, I. Mateo Leach, W. L. McArdle, S. A. McCarroll, S. E. Medland, K. A. Miller, G. W. Montgomery, A. C. Morrison, M. Muller-Nurasyid, P. Navarro, M. Nelis, J. R. O'Connell, C. J. O'Donnell, K. K. Ong, A. B. Newman, A. Peters, O. Polasek, A. Pouta, P. P. Pramstaller, B. M. Psaty, D. C. Rao, S. M. Ring, E. J. Rossin, D. Rudan, S. Sanna, R. A. Scott, J. S. Sehmi, S. Sharp, J. T. Shin, A. B. Singleton, A. V. Smith, N. Soranzo, T. D. Spector, C. Stewart, H. M. Stringham, K. V. Tarasov, A. G. Uitterlinden, L. Vandenput, S. J. Hwang, J. B. Whitfield, C. Wijmenga, S. H. Wild, G. Willemsen, J. F. Wilson, J. C. Witteman, A. Wong, Q. Wong, Y. Jamshidi, P. Zitting, J. M. Boer, D. I. Boomsma, I. B. Borecki, C. M. van Duijn, U. Ekelund, N. G. Forouhi, P. Froguel, A. Hingorani, E. Ingelsson, M. Kivimaki, R. A. Kronmal, D. Kuh, L. Lind, N. G. Martin, B. A. Oostra, N. L. Pedersen, T. Quertermous, J. I. Rotter, Y. T. van der Schouw, W. M. Verschuren, M. Walker, D. Albanes, D. O. Arnar, T. L. Assimes, S. Bandinelli, M. Boehnke, R. A. de Boer, C. Bouchard, W. L. Caulfield, J. C. Chambers, G. Curhan, D. Cusi, J. Eriksson, L. Ferrucci, W. H. van Gilst, N. Glorioso, J. de Graaf, L. Groop, U. Gyllensten, W. C. Hsueh, F. B. Hu, H. V. Huikuri, D. J. Hunter, C. Iribarren, B. Isomaa, M. R. Jarvelin, A. Jula, M. Kahonen, L. A. Kiemeney, M. M. van der Klauw, J. S. Kooner, P. Kraft, L. Iacoviello, T. Lehtimaki, M. L. Lokki, B. D. Mitchell, G. Navis, M. S. Nieminen, C. Ohlsson, N. R. Poulter, L. Qi, O. T. Raitakari, E. B. Rimm, J. D. Rioux, F. Rizzi, I. Rudan, V. Salomaa, P. S. Sever, D. C. Shields, A. R. Shuldiner, J. Sinisalo, A. V. Stanton, R. P. Stolk, D. P. Strachan, J. C. Tardif, U. Thorsteinsdottir, J. Tuomilehto, D. J. van Veldhuisen, J. Virtamo, J. Viikari, P. Vollenweider, G. Waeber, E. Widen, Y. S. Cho, J. V. Olsen, P. M. Visscher, C. Willer, L. Franke, Global BPgen Consortium, CARDIoGRAM Consortium, J. Erdmann, J. R. Thompson, PR GWAS Consortium, A. Pfeufer, QRS GWAS Consortium, N. Sotoodehnia, QT-IGC Consortium, C. Newton-Cheh, Charge-AF Consortium, P. T. Ellinor, B. H. Stricker, A. Metspalu, M. Perola, J. S. Beckmann, G. D. Smith, K. Stefansson, N. J. Wareham, P. B. Munroe, O. C. Sibon, D. J. Milan, H. Snieder, N. J. Samani, R. J. Loos, Identification of heart rate-associated loci and their effects on cardiac conduction and rhythm disorders. *Nat. Genet.* **45**, 621-631 (2013).

6. R. F. Gillum, D. M. Makuc, J. J. Feldman, Pulse rate, coronary heart disease, and death: the NHANES I Epidemiologic Follow-up Study. *Am. Heart J.* **121**, 172-177 (1991).
7. J. Nauman, I. Janszky, L. J. Vatten, U. Wisloff, Temporal changes in resting heart rate and deaths from ischemic heart disease. *JAMA* **306**, 2579-2587 (2011).
8. K. L. Poon, T. Brand, The zebrafish model system in cardiovascular research: A tiny fish with mighty prospects. *Glob Cardiol Sci Pract* **2013**, 9-28 (2013).
9. R. N. Eppinga, Y. Hagemeijer, S. Burgess, D. A. Hinds, K. Stefansson, D. F. Gudbjartsson, D. J. van Veldhuisen, P. B. Munroe, N. Verweij, P. van der Harst, Identification of genomic loci associated with resting heart rate and shared genetic predictors with all-cause mortality. *Nat. Genet.* **48**, 1557-1563 (2016).
10. D. E. Arking, S. L. Pulit, L. Crotti, P. van der Harst, P. B. Munroe, T. T. Koopmann, N. Sotoodehnia, E. J. Rossin, M. Morley, X. Wang, A. D. Johnson, A. Lundby, D. F. Gudbjartsson, P. A. Noseworthy, M. Eijgelsheim, Y. Bradford, K. V. Tarasov, M. Dorr, M. Muller-Nurasyid, A. M. Lahtinen, I. M. Nolte, A. V. Smith, J. C. Bis, A. Isaacs, S. J. Newhouse, D. S. Evans, W. S. Post, D. Waggott, L. P. Lyytikainen, A. A. Hicks, L. Eisele, D. Ellinghaus, C. Hayward, P. Navarro, S. Ulivi, T. Tanaka, D. J. Tester, S. Chatel, S. Gustafsson, M. Kumari, R. W. Morris, A. T. Naluai, S. Padmanabhan, A. Kluttig, B. Strohmer, A. G. Panayiotou, M. Torres, M. Knoflach, J. A. Hubacek, K. Slowikowski, S. Raychaudhuri, R. D. Kumar, T. B. Harris, L. J. Launer, A. R. Shuldiner, A. Alonso, J. S. Bader, G. Ehret, H. Huang, W. H. Kao, J. B. Strait, P. W. Macfarlane, M. Brown, M. J. Caulfield, N. J. Samani, F. Kronenberg, J. Willeit, CARe Consortium, COGENT Consortium, J. G. Smith, K. H. Greiser, H. Meyer Zu Schwabedissen, K. Werdan, M. Carella, L. Zelante, S. R. Heckbert, B. M. Psaty, J. I. Rotter, I. Kolcic, O. Polasek, A. F. Wright, M. Griffin, M. J. Daly, Dcct/Edic, D. O. Arnar, H. Holm, U. Thorsteinsdottir, eMerge Consortium, J. C. Denny, D. M. Roden, R. L. Zuvich, V. Emilsson, A. S. Plump, M. G. Larson, C. J. O'Donnell, X. Yin, M. Bobbo, A. P. D'Adamo, A. Iorio, G. Sinagra, A. Carracedo, S. R. Cummings, M. A. Nalls, A. Jula, K. K. Kontula, A. Marjamaa, L. Oikarinen, M. Perola, K. Porthan, R. Erbel, P. Hoffmann, K. H. Jockel, H. Kalsch, M. M. Nothen, HRGEN Consortium, M. den Hoed, R. J. Loos, D. S. Thelle, C. Gieger, T. Meitinger, S. Perz, A. Peters, H. Prucha, M. F. Sinner, M. Waldenberger, R. A. de Boer, L. Franke, P. A. van der Vleuten, B. M. Beckmann, E. Martens, A. Bardai, N. Hofman, A. A. Wilde, E. R. Behr, C. Dalageorgou, J. R. Giudicessi, A. Medeiros-Domingo, J. Barc, F. Kyndt, V. Probst, A. Ghidoni, R. Insolia, R. M. Hamilton, S. W. Scherer, J. Brandimarto, K. Margulies, C. E. Moravec, M. F. del Greco, C. Fuchsberger, J. R. O'Connell, W. K. Lee, G. C. Watt, H. Campbell, S. H. Wild, N. E. El Mokhtari, N. Frey, F. W. Asselbergs, I. Mateo Leach, G. Navis, M. P. van den Berg, D. J. van Veldhuisen, M. Kellis, B. P. Krijthe, O. H. Franco, A. Hofman, J. A. Kors, A. G. Uitterlinden, J. C. Witteman, L. Kedenko, C. Lamina, B. A. Oostra, G. R. Abecasis, E. G. Lakatta, A. Mulas, M. Orru, D. Schlessinger, M. Uda, M. R. Markus, U. Volker, H. Snieder, T. D. Spector, J. Arnlov, L. Lind, J. Sundstrom, A. C. Syvanen, M. Kivimaki, M. Kahonen, N. Mononen, O. T. Raitakari, J. S. Viikari, V.

Adamkova, S. Kiechl, M. Brion, A. N. Nicolaides, B. Paulweber, J. Haerting, A. F. Dominiczak, F. Nyberg, P. H. Whincup, A. D. Hingorani, J. J. Schott, C. R. Bezzina, E. Ingelsson, L. Ferrucci, P. Gasparini, J. F. Wilson, I. Rudan, A. Franke, T. W. Muhleisen, P. P. Pramstaller, T. J. Lehtimaki, A. D. Paterson, A. Parsa, Y. Liu, C. M. van Duijn, D. S. Siscovick, V. Gudnason, Y. Jamshidi, V. Salomaa, S. B. Felix, S. Sanna, M. D. Ritchie, B. H. Stricker, K. Stefansson, L. A. Boyer, T. P. Cappola, J. V. Olsen, K. Lage, P. J. Schwartz, S. Kaab, A. Chakravarti, M. J. Ackerman, A. Pfeufer, P. I. de Bakker, C. Newton-Cheh, Genetic association study of QT interval highlights role for calcium signaling pathways in myocardial repolarization. *Nat. Genet.* **46**, 826-836 (2014).

11. G. J. Lieschke, P. D. Currie, Animal models of human disease: zebrafish swim into view. *Nat Rev Genet* **8**, 353-367 (2007).
12. C. A. MacRae, R. T. Peterson, Zebrafish as tools for drug discovery. *Nat Rev Drug Discov* **14**, 721-731 (2015).
13. C. C. Liu, L. Li, Y. W. Lam, C. W. Siu, S. H. Cheng, Improvement of surface ECG recording in adult zebrafish reveals that the value of this model exceeds our expectation. *Sci. Rep.* **6**, 25073 (2016).
14. C. Pardo-Martin, A. Allalou, J. Medina, P. M. Eimon, C. Wahlby, M. Fatih Yanik, High-throughput hyperdimensional vertebrate phenotyping. *Nat Commun* **4**, 1467 (2013).
15. K. Howe, M. D. Clark, C. F. Torroja, J. Torrance, C. Berthelot, M. Muffato, J. E. Collins, S. Humphray, K. McLaren, L. Matthews, S. McLaren, I. Sealy, M. Caccamo, C. Churcher, C. Scott, J. C. Barrett, R. Koch, G. J. Rauch, S. White, W. Chow, B. Kilian, L. T. Quintais, J. A. Guerra-Assuncao, Y. Zhou, Y. Gu, J. Yen, J. H. Vogel, T. Eyre, S. Redmond, R. Banerjee, J. Chi, B. Fu, E. Langley, S. F. Maguire, G. K. Laird, D. Lloyd, E. Kenyon, S. Donaldson, H. Sehra, J. Almeida-King, J. Loveland, S. Trevanion, M. Jones, M. Quail, D. Willey, A. Hunt, J. Burton, S. Sims, K. McLay, B. Plumb, J. Davis, C. Clee, K. Oliver, R. Clark, C. Riddle, D. Elliot, G. Threadgold, G. Harden, D. Ware, S. Begum, B. Mortimore, G. Kerry, P. Heath, B. Phillimore, A. Tracey, N. Corby, M. Dunn, C. Johnson, J. Wood, S. Clark, S. Pelan, G. Griffiths, M. Smith, R. Glithero, P. Howden, N. Barker, C. Lloyd, C. Stevens, J. Harley, K. Holt, G. Panagiotidis, J. Lovell, H. Beasley, C. Henderson, D. Gordon, K. Auger, D. Wright, J. Collins, C. Raisen, L. Dyer, K. Leung, L. Robertson, K. Ambridge, D. Leongamornlert, S. McGuire, R. Gilderthorp, C. Griffiths, D. Manthravadi, S. Nichol, G. Barker, S. Whitehead, M. Kay, J. Brown, C. Murnane, E. Gray, M. Humphries, N. Sycamore, D. Barker, D. Saunders, J. Wallis, A. Babbage, S. Hammond, M. Mashreghi-Mohammadi, L. Barr, S. Martin, P. Wray, A. Ellington, N. Matthews, M. Ellwood, R. Woodmansey, G. Clark, J. Cooper, A. Tromans, D. Grafham, C. Skuce, R. Pandian, R. Andrews, E. Harrison, A. Kimberley, J. Garnett, N. Fosker, R. Hall, P. Garner, D. Kelly, C. Bird, S. Palmer, I. Gehring, A. Berger, C. M. Dooley, Z. Ersan-Urun, C. Eser, H. Geiger, M. Geisler, L. Karotki, A. Kirn, J. Konantz, M. Konantz, M. Oberlander, S. Rudolph-Geiger, M. Teucke, C. Lanz, G. Raddatz, K. Osoegawa, B. Zhu, A. Rapp, S. Widaa, C. Langford, F. Yang, S. C. Schuster, N. P. Carter, J. Harrow, Z. Ning, J. Herrero, S. M. Searle, A. Enright, R. Geisler, R. H. Plasterk, C. Lee, M. Westerfield, P. J. de Jong, L. I. Zon, J. H. Postlethwait, C. Nusslein-Volhard, T. J. Hubbard, H. Roest Crollius, J.

Rogers, D. L. Stemple, The zebrafish reference genome sequence and its relationship to the human genome. *Nature* **496**, 498-503 (2013).
16. G. K. Varshney, B. Carrington, W. Pei, K. Bishop, Z. Chen, C. Fan, L. Xu, M. Jones, M. C. LaFave, J. Ledin, R. Sood, S. M. Burgess, A high-throughput functional genomics workflow based on CRISPR/Cas9-mediated targeted mutagenesis in zebrafish. *Nat. Protoc.* **11**, 2357-2375 (2016).
17. J. H. Hou, J. M. Kralj, A. D. Douglass, F. Engert, A. E. Cohen, Simultaneous mapping of membrane voltage and calcium in zebrafish heart in vivo reveals chamber-specific developmental transitions in ionic currents. *Front. Physiol.* **5**, 344 (2014).
18. K. C. Cotto, A. H. Wagner, Y. Y. Feng, S. Kiwala, A. C. Coffman, G. Spies, A. Wollam, N. C. Spies, O. L. Griffith, M. Griffith, DGIdb 3.0: a redesign and expansion of the drug-gene interaction database. *Nucleic Acids Res.* **46**, D1068-D1073 (2018).
19. M. Böhm, K. Swedberg, M. Komajda, J. S. Borer, I. Ford, A. Dubost-Brama, G. Lerebours, L. Tavazzi, Heart rate as a risk factor in chronic heart failure (SHIFT): the association between heart rate and outcomes in a randomised placebo-controlled trial. *The Lancet* **376**, 886-894 (2010).
20. D. Warde-Farley, S. L. Donaldson, O. Comes, K. Zuberi, R. Badrawi, P. Chao, M. Franz, C. Grouios, F. Kazi, C. T. Lopes, A. Maitland, S. Mostafavi, J. Montojo, Q. Shao, G. Wright, G. D. Bader, Q. Morris, The GeneMANIA prediction server: biological network integration for gene prioritization and predicting gene function. *Nucleic Acids Res.* **38**, W214-220 (2010).
21. D. Szklarczyk, J. H. Morris, H. Cook, M. Kuhn, S. Wyder, M. Simonovic, A. Santos, N. T. Doncheva, A. Roth, P. Bork, L. J. Jensen, C. von Mering, The STRING database in 2017: quality-controlled protein-protein association networks, made broadly accessible. *Nucleic Acids Res.* **45**, D362-d368 (2017).
22. A. Battle, C. D. Brown, B. E. Engelhardt, S. B. Montgomery, Genetic effects on gene expression across human tissues. *Nature* **550**, 204-213 (2017).
23. D. Lagman, G. Sundstrom, D. Ocampo Daza, X. M. Abalo, D. Larhammar, Expansion of transducin subunit gene families in early vertebrate tetraploidizations. *Genomics* **100**, 203-211 (2012).
24. M. D. Mark, S. Herlitze, G-protein mediated gating of inward-rectifier K+ channels. *Eur. J. Biochem.* **267**, 5830-5836 (2000).
25. J. Bakkers, Zebrafish as a model to study cardiac development and human cardiac disease. *Cardiovasc. Res.* **91**, 279-288 (2011).
26. T. C. Sudhof, Synaptotagmins: why so many? *J. Biol. Chem.* **277**, 7629-7632 (2002).
27. E. R. Chapman, How does synaptotagmin trigger neurotransmitter release? *Annu. Rev. Biochem.* **77**, 615-641 (2008).
28. P. T. Ellinor, K. L. Lunetta, C. M. Albert, N. L. Glazer, M. D. Ritchie, A. V. Smith, D. E. Arking, M. Muller-Nurasyid, B. P. Krijthe, S. A. Lubitz, J. C. Bis, M. K. Chung, M. Dorr, K. Ozaki, J. D. Roberts, J. G. Smith, A. Pfeufer, M. F. Sinner, K. Lohman, J. Ding, N. L. Smith, J. D. Smith, M. Rienstra, K. M. Rice, D. R. Van Wagoner, J. W. Magnani, R. Wakili, S. Clauss, J. I. Rotter, G. Steinbeck, L. J. Launer, R. W. Davies, M. Borkovich, T. B. Harris, H. Lin, U. Volker, H. Volzke, D. J. Milan, A. Hofman, E. Boerwinkle, L. Y. Chen, E. Z. Soliman, B. F. Voight, G. Li, A. Chakravarti, M. Kubo, U. B. Tedrow, L. M.

Rose, P. M. Ridker, D. Conen, T. Tsunoda, T. Furukawa, N. Sotoodehnia, S. Xu, N. Kamatani, D. Levy, Y. Nakamura, B. Parvez, S. Mahida, K. L. Furie, J. Rosand, R. Muhammad, B. M. Psaty, T. Meitinger, S. Perz, H. E. Wichmann, J. C. Witteman, W. H. Kao, S. Kathiresan, D. M. Roden, A. G. Uitterlinden, F. Rivadeneira, B. McKnight, M. Sjogren, A. B. Newman, Y. Liu, M. H. Gollob, O. Melander, T. Tanaka, B. H. Stricker, S. B. Felix, A. Alonso, D. Darbar, J. Barnard, D. I. Chasman, S. R. Heckbert, E. J. Benjamin, V. Gudnason, S. Kaab, Meta-analysis identifies six new susceptibility loci for atrial fibrillation. *Nat. Genet.* **44**, 670-675 (2012).

29. W. Shi, R. Wymore, H. Yu, J. Wu, R. T. Wymore, Z. Pan, R. B. Robinson, J. E. Dixon, D. McKinnon, I. S. Cohen, Distribution and prevalence of hyperpolarization-activated cation channel (HCN) mRNA expression in cardiac tissues. *Circ. Res.* **85**, e1-6 (1999).
30. A. Ludwig, X. Zong, J. Stieber, R. Hullin, F. Hofmann, M. Biel, Two pacemaker channels from human heart with profoundly different activation kinetics. *EMBO J.* **18**, 2323-2329 (1999).
31. J. Stieber, S. Herrmann, S. Feil, J. Loster, R. Feil, M. Biel, F. Hofmann, A. Ludwig, The hyperpolarization-activated channel HCN4 is required for the generation of pacemaker action potentials in the embryonic heart. *Proc. Natl. Acad. Sci. U. S. A.* **100**, 15235-15240 (2003).
32. A. Bucchi, M. Baruscotti, M. Nardini, A. Barbuti, S. Micheloni, M. Bolognesi, D. DiFrancesco, Identification of the molecular site of ivabradine binding to HCN4 channels. *PLoS One* **8**, e53132 (2013).
33. K. Swedberg, M. Komajda, M. Bohm, J. S. Borer, I. Ford, A. Dubost-Brama, G. Lerebours, L. Tavazzi, Ivabradine and outcomes in chronic heart failure (SHIFT): a randomised placebo-controlled study. *Lancet* **376**, 875-885 (2010).
34. W. W. Burggren, A. W. Pinder, Ontogeny of cardiovascular and respiratory physiology in lower vertebrates. *Annu. Rev. Physiol.* **53**, 107-135 (1991).
35. N. H. Wilson, B. Key, Neogenin: one receptor, many functions. *Int. J. Biochem. Cell Biol.* **39**, 874-878 (2007).
36. D. J. Mawdsley, H. M. Cooper, B. M. Hogan, S. H. Cody, G. J. Lieschke, J. K. Heath, The Netrin receptor Neogenin is required for neural tube formation and somitogenesis in zebrafish. *Dev. Biol.* **269**, 302-315 (2004).
37. J. Stieber, K. Wieland, G. Stockl, A. Ludwig, F. Hofmann, Bradycardic and proarrhythmic properties of sinus node inhibitors. *Mol. Pharmacol.* **69**, 1328-1337 (2006).
38. C. Newton-Cheh, C. Y. Guo, T. J. Wang, J. O'Donnell C, D. Levy, M. G. Larson, Genome-wide association study of electrocardiographic and heart rate variability traits: the Framingham Heart Study. *BMC Med. Genet.* **8 Suppl 1**, S7 (2007).
39. C. Dong, D. Della-Morte, A. Beecham, L. Wang, D. Cabral, S. H. Blanton, R. L. Sacco, T. Rundek, Genetic variants in LEKR1 and GALNT10 modulate sex-difference in carotid intima-media thickness: a genome-wide interaction study. *Atherosclerosis* **240**, 462-467 (2015).
40. A. E. Locke, B. Kahali, S. I. Berndt, A. E. Justice, T. H. Pers, F. R. Day, C. Powell, S. Vedantam, M. L. Buchkovich, J. Yang, D. C. Croteau-Chonka, T. Esko, T. Fall, T. Ferreira, S. Gustafsson, Z. Kutalik, J. Luan, R. Magi, J. C. Randall, T. W. Winkler, A. R. Wood, T. Workalemahu, J. D. Faul, J. A. Smith,

J. H. Zhao, W. Zhao, J. Chen, R. Fehrmann, A. K. Hedman, J. Karjalainen, E. M. Schmidt, D. Absher, N. Amin, D. Anderson, M. Beekman, J. L. Bolton, J. L. Bragg-Gresham, S. Buyske, A. Demirkan, G. Deng, G. B. Ehret, B. Feenstra, M. F. Feitosa, K. Fischer, A. Goel, J. Gong, A. U. Jackson, S. Kanoni, M. E. Kleber, K. Kristiansson, U. Lim, V. Lotay, M. Mangino, I. M. Leach, C. Medina-Gomez, S. E. Medland, M. A. Nalls, C. D. Palmer, D. Pasko, S. Pechlivanis, M. J. Peters, I. Prokopenko, D. Shungin, A. Stancakova, R. J. Strawbridge, Y. J. Sung, T. Tanaka, A. Teumer, S. Trompet, S. W. van der Laan, J. van Setten, J. V. Van Vliet-Ostaptchouk, Z. Wang, L. Yengo, W. Zhang, A. Isaacs, E. Albrecht, J. Arnlov, G. M. Arscott, A. P. Attwood, S. Bandinelli, A. Barrett, I. N. Bas, C. Bellis, A. J. Bennett, C. Berne, R. Blagieva, M. Bluher, S. Bohringer, L. L. Bonnycastle, Y. Bottcher, H. A. Boyd, M. Bruinenberg, I. H. Caspersen, Y. I. Chen, R. Clarke, E. W. Daw, A. J. M. de Craen, G. Delgado, M. Dimitriou, A. S. F. Doney, N. Eklund, K. Estrada, E. Eury, L. Folkersen, R. M. Fraser, M. E. Garcia, F. Geller, V. Giedraitis, B. Gigante, A. S. Go, A. Golay, A. H. Goodall, S. D. Gordon, M. Gorski, H. J. Grabe, H. Grallert, T. B. Grammer, J. Grassler, H. Gronberg, C. J. Groves, G. Gusto, J. Haessler, P. Hall, T. Haller, G. Hallmans, C. A. Hartman, M. Hassinen, C. Hayward, N. L. Heard-Costa, Q. Helmer, C. Hengstenberg, O. Holmen, J. J. Hottenga, A. L. James, J. M. Jeff, A. Johansson, J. Jolley, T. Juliusdottir, L. Kinnunen, W. Koenig, M. Koskenvuo, W. Kratzer, J. Laitinen, C. Lamina, K. Leander, N. R. Lee, P. Lichtner, L. Lind, J. Lindstrom, K. S. Lo, S. Lobbens, R. Lorbeer, Y. Lu, F. Mach, P. K. E. Magnusson, A. Mahajan, W. L. McArdle, S. McLachlan, C. Menni, S. Merger, E. Mihailov, L. Milani, A. Moayyeri, K. L. Monda, M. A. Morken, A. Mulas, G. Muller, M. Muller-Nurasyid, A. W. Musk, R. Nagaraja, M. M. Nothen, I. M. Nolte, S. Pilz, N. W. Rayner, F. Renstrom, R. Rettig, J. S. Ried, S. Ripke, N. R. Robertson, L. M. Rose, S. Sanna, H. Scharnagl, S. Scholtens, F. R. Schumacher, W. R. Scott, T. Seufferlein, J. Shi, A. V. Smith, J. Smolonska, A. V. Stanton, V. Steinthorsdottir, K. Stirrups, H. M. Stringham, J. Sundstrom, M. A. Swertz, A. J. Swift, A. C. Syvanen, S. T. Tan, B. O. Tayo, B. Thorand, G. Thorleifsson, J. P. Tyrer, H. W. Uh, L. Vandenput, F. C. Verhulst, S. H. Vermeulen, N. Verweij, J. M. Vonk, L. L. Waite, H. R. Warren, D. Waterworth, M. N. Weedon, L. R. Wilkens, C. Willenborg, T. Wilsgaard, M. K. Wojczynski, A. Wong, A. F. Wright, Q. Zhang, E. P. Brennan, M. Choi, Z. Dastani, A. W. Drong, P. Eriksson, A. Franco-Cereceda, J. R. Gadin, A. G. Gharavi, M. E. Goddard, R. E. Handsaker, J. Huang, F. Karpe, S. Kathiresan, S. Keildson, K. Kiryluk, M. Kubo, J. Y. Lee, L. Liang, R. P. Lifton, B. Ma, S. A. McCarroll, A. J. McKnight, J. L. Min, M. F. Moffatt, G. W. Montgomery, J. M. Murabito, G. Nicholson, D. R. Nyholt, Y. Okada, J. R. B. Perry, R. Dorajoo, E. Reinmaa, R. M. Salem, N. Sandholm, R. A. Scott, L. Stolk, A. Takahashi, F. M. van 't Hooft, A. A. E. Vinkhuyzen, H. J. Westra, W. Zheng, K. T. Zondervan, A. C. Heath, D. Arveiler, S. J. L. Bakker, J. Beilby, R. N. Bergman, J. Blangero, P. Bovet, H. Campbell, M. J. Caulfield, G. Cesana, A. Chakravarti, D. I. Chasman, P. S. Chines, F. S. Collins, D. C. Crawford, L. A. Cupples, D. Cusi, J. Danesh, U. de Faire, H. M. den Ruijter, A. F. Dominiczak, R. Erbel, J. Erdmann, J. G. Eriksson, M. Farrall, S. B. Felix, E. Ferrannini, J. Ferrieres, I. Ford, N. G. Forouhi, T. Forrester, O. H. Franco, R. T. Gansevoort, P. V. Gejman, C. Gieger, O. Gottesman, V. Gudnason, U. Gyllensten, A. S. Hall, T. B. Harris, A.

T. Hattersley, A. A. Hicks, L. A. Hindorff, A. D. Hingorani, A. Hofman, G. Homuth, G. K. Hovingh, S. E. Humphries, S. C. Hunt, E. Hypponen, T. Illig, K. B. Jacobs, M. R. Jarvelin, K. H. Jockel, B. Johansen, P. Jousilahti, J. W. Jukema, A. M. Jula, J. Kaprio, J. J. P. Kastelein, S. M. Keinanen-Kiukaanniemi, L. A. Kiemeney, P. Knekt, J. S. Kooner, C. Kooperberg, P. Kovacs, A. T. Kraja, M. Kumari, J. Kuusisto, T. A. Lakka, C. Langenberg, L. L. Marchand, T. Lehtimaki, V. Lyssenko, S. Mannisto, A. Marette, T. C. Matise, C. A. McKenzie, B. McKnight, F. L. Moll, A. D. Morris, A. P. Morris, J. C. Murray, M. Nelis, C. Ohlsson, A. J. Oldehinkel, K. K. Ong, P. A. F. Madden, G. Pasterkamp, J. F. Peden, A. Peters, D. S. Postma, P. P. Pramstaller, J. F. Price, L. Qi, O. T. Raitakari, T. Rankinen, D. C. Rao, T. K. Rice, P. M. Ridker, J. D. Rioux, M. D. Ritchie, I. Rudan, V. Salomaa, N. J. Samani, J. Saramies, M. A. Sarzynski, H. Schunkert, P. E. H. Schwarz, P. Sever, A. R. Shuldiner, J. Sinisalo, R. P. Stolk, K. Strauch, A. Tonjes, D. A. Tregouet, A. Tremblay, E. Tremoli, J. Virtamo, M. C. Vohl, U. Volker, G. Waeber, G. Willemsen, J. C. Witteman, M. C. Zillikens, L. S. Adair, P. Amouyel, F. W. Asselbergs, T. L. Assimes, M. Bochud, B. O. Boehm, E. Boerwinkle, S. R. Bornstein, E. P. Bottinger, C. Bouchard, S. Cauchi, J. C. Chambers, S. J. Chanock, R. S. Cooper, P. I. W. de Bakker, G. Dedoussis, L. Ferrucci, P. W. Franks, P. Froguel, L. C. Groop, C. A. Haiman, A. Hamsten, J. Hui, D. J. Hunter, K. Hveem, R. C. Kaplan, M. Kivimaki, D. Kuh, M. Laakso, Y. Liu, N. G. Martin, W. Marz, M. Melbye, A. Metspalu, S. Moebus, P. B. Munroe, I. Njolstad, B. A. Oostra, C. N. A. Palmer, N. L. Pedersen, M. Perola, L. Perusse, U. Peters, C. Power, T. Quertermous, R. Rauramaa, F. Rivadeneira, T. E. Saaristo, D. Saleheen, N. Sattar, E. E. Schadt, D. Schlessinger, P. E. Slagboom, H. Snieder, T. D. Spector, U. Thorsteinsdottir, M. Stumvoll, J. Tuomilehto, A. G. Uitterlinden, M. Uusitupa, P. van der Harst, M. Walker, H. Wallaschofski, N. J. Wareham, H. Watkins, D. R. Weir, H. E. Wichmann, J. F. Wilson, P. Zanen, I. B. Borecki, P. Deloukas, C. S. Fox, I. M. Heid, J. R. O'Connell, D. P. Strachan, K. Stefansson, C. M. van Duijn, G. R. Abecasis, L. Franke, T. M. Frayling, M. I. McCarthy, P. M. Visscher, A. Scherag, C. J. Willer, M. Boehnke, K. L. Mohlke, C. M. Lindgren, J. S. Beckmann, I. Barroso, K. E. North, E. Ingelsson, J. N. Hirschhorn, R. J. F. Loos, E. K. Speliotes, Genetic studies of body mass index yield new insights for obesity biology. *Nature* **518**, 197-206 (2015).

41. A. E. Justice, T. W. Winkler, M. F. Feitosa, M. Graff, V. A. Fisher, K. Young, L. Barata, X. Deng, J. Czajkowski, D. Hadley, J. S. Ngwa, T. S. Ahluwalia, A. Y. Chu, N. L. Heard-Costa, E. Lim, J. Perez, J. D. Eicher, Z. Kutalik, L. Xue, A. Mahajan, F. Renstrom, J. Wu, Q. Qi, S. Ahmad, T. Alfred, N. Amin, L. F. Bielak, A. Bonnefond, J. Bragg, G. Cadby, M. Chittani, S. Coggeshall, T. Corre, N. Direk, J. Eriksson, K. Fischer, M. Gorski, M. Neergaard Harder, M. Horikoshi, T. Huang, J. E. Huffman, A. U. Jackson, J. M. Justesen, S. Kanoni, L. Kinnunen, M. E. Kleber, P. Komulainen, M. Kumari, U. Lim, J. Luan, L. P. Lyytikainen, M. Mangino, A. Manichaikul, J. Marten, R. P. S. Middelberg, M. Muller-Nurasyid, P. Navarro, L. Perusse, N. Pervjakova, C. Sarti, A. V. Smith, J. A. Smith, A. Stancakova, R. J. Strawbridge, H. M. Stringham, Y. J. Sung, T. Tanaka, A. Teumer, S. Trompet, S. W. van der Laan, P. J. van der Most, J. V. Van Vliet-Ostaptchouk, S. L. Vedantam, N. Verweij, J. M. Vink, V. Vitart, Y. Wu, L. Yengo, W. Zhang, J. Hua Zhao, M. E. Zimmermann, N. Zubair, G. R. Abecasis, L. S. Adair, S. Afaq, U. Afzal, S. J. L. Bakker, T. M.

Bartz, J. Beilby, R. N. Bergman, S. Bergmann, R. Biffar, J. Blangero, E. Boerwinkle, L. L. Bonnycastle, E. Bottinger, D. Braga, B. M. Buckley, S. Buyske, H. Campbell, J. C. Chambers, F. S. Collins, J. E. Curran, G. J. de Borst, A. J. M. de Craen, E. J. C. de Geus, G. Dedoussis, G. E. Delgado, H. M. den Ruijter, G. Eiriksdottir, A. L. Eriksson, T. Esko, J. D. Faul, I. Ford, T. Forrester, K. Gertow, B. Gigante, N. Glorioso, J. Gong, H. Grallert, T. B. Grammer, N. Grarup, S. Haitjema, G. Hallmans, A. Hamsten, T. Hansen, T. B. Harris, C. A. Hartman, M. Hassinen, N. D. Hastie, A. C. Heath, D. Hernandez, L. Hindorff, L. J. Hocking, M. Hollensted, O. L. Holmen, G. Homuth, J. Jan Hottenga, J. Huang, J. Hung, N. Hutri-Kahonen, E. Ingelsson, A. L. James, J. O. Jansson, M. R. Jarvelin, M. A. Jhun, M. E. Jorgensen, M. Juonala, M. Kahonen, M. Karlsson, H. A. Koistinen, I. Kolcic, G. Kolovou, C. Kooperberg, B. K. Kramer, J. Kuusisto, K. Kvaloy, T. A. Lakka, C. Langenberg, L. J. Launer, K. Leander, N. R. Lee, L. Lind, C. M. Lindgren, A. Linneberg, S. Lobbens, M. Loh, M. Lorentzon, R. Luben, G. Lubke, A. Ludolph-Donislawski, S. Lupoli, P. A. F. Madden, R. Mannikko, P. Marques-Vidal, N. G. Martin, C. A. McKenzie, B. McKnight, D. Mellstrom, C. Menni, G. W. Montgomery, A. B. Musk, N. Narisu, M. Nauck, I. M. Nolte, A. J. Oldehinkel, M. Olden, K. K. Ong, S. Padmanabhan, P. A. Peyser, C. Pisinger, D. J. Porteous, O. T. Raitakari, T. Rankinen, D. C. Rao, L. J. Rasmussen-Torvik, R. Rawal, T. Rice, P. M. Ridker, L. M. Rose, S. A. Bien, I. Rudan, S. Sanna, M. A. Sarzynski, N. Sattar, K. Savonen, D. Schlessinger, S. Scholtens, C. Schurmann, R. A. Scott, B. Sennblad, M. A. Siemelink, G. Silbernagel, P. E. Slagboom, H. Snieder, J. A. Staessen, D. J. Stott, M. A. Swertz, A. J. Swift, K. D. Taylor, B. O. Tayo, B. Thorand, D. Thuillier, J. Tuomilehto, A. G. Uitterlinden, L. Vandenput, M. C. Vohl, H. Volzke, J. M. Vonk, G. Waeber, M. Waldenberger, R. G. J. Westendorp, S. Wild, G. Willemsen, B. H. R. Wolffenbuttel, A. Wong, A. F. Wright, W. Zhao, M. C. Zillikens, D. Baldassarre, B. Balkau, S. Bandinelli, C. A. Boger, D. I. Boomsma, C. Bouchard, M. Bruinenberg, D. I. Chasman, Y. D. Chen, P. S. Chines, R. S. Cooper, F. Cucca, D. Cusi, U. Faire, L. Ferrucci, P. W. Franks, P. Froguel, P. Gordon-Larsen, H. J. Grabe, V. Gudnason, C. A. Haiman, C. Hayward, K. Hveem, A. D. Johnson, J. Wouter Jukema, S. L. R. Kardia, M. Kivimaki, J. S. Kooner, D. Kuh, M. Laakso, T. Lehtimaki, L. L. Marchand, W. Marz, M. I. McCarthy, A. Metspalu, A. P. Morris, C. Ohlsson, L. J. Palmer, G. Pasterkamp, O. Pedersen, A. Peters, U. Peters, O. Polasek, B. M. Psaty, L. Qi, R. Rauramaa, B. H. Smith, T. I. A. Sorensen, K. Strauch, H. Tiemeier, E. Tremoli, P. van der Harst, H. Vestergaard, P. Vollenweider, N. J. Wareham, D. R. Weir, J. B. Whitfield, J. F. Wilson, J. Tyrrell, T. M. Frayling, I. Barroso, M. Boehnke, P. Deloukas, C. S. Fox, J. N. Hirschhorn, D. J. Hunter, T. D. Spector, D. P. Strachan, C. M. van Duijn, I. M. Heid, K. L. Mohlke, J. Marchini, R. J. F. Loos, T. O. Kilpelainen, C. T. Liu, I. B. Borecki, K. E. North, L. A. Cupples, Genome-wide meta-analysis of 241,258 adults accounting for smoking behaviour identifies novel loci for obesity traits. *Nat Commun* **8**, 14977 (2017).

42. M. C. Y. Ng, M. Graff, Y. Lu, A. E. Justice, P. Mudgal, C. T. Liu, K. Young, L. R. Yanek, M. F. Feitosa, M. K. Wojczynski, K. Rand, J. A. Brody, B. E. Cade, L. Dimitrov, Q. Duan, X. Guo, L. A. Lange, M. A. Nalls, H. Okut, S. M. Tajuddin, B. O. Tayo, S. Vedantam, J. P. Bradfield, G. Chen, W. M. Chen, A. Chesi, M. R. Irvin, B. Padhukasahasram, J. A. Smith, W. Zheng, M. A. Allison, C. B.

Ambrosone, E. V. Bandera, T. M. Bartz, S. I. Berndt, L. Bernstein, W. J. Blot, E. P. Bottinger, J. Carpten, S. J. Chanock, Y. I. Chen, D. V. Conti, R. S. Cooper, M. Fornage, B. I. Freedman, M. Garcia, P. J. Goodman, Y. H. Hsu, J. Hu, C. D. Huff, S. A. Ingles, E. M. John, R. Kittles, E. Klein, J. Li, B. McKnight, U. Nayak, B. Nemesure, A. Ogunniyi, A. Olshan, M. F. Press, R. Rohde, B. A. Rybicki, B. Salako, M. Sanderson, Y. Shao, D. S. Siscovick, J. L. Stanford, V. L. Stevens, A. Stram, S. S. Strom, D. Vaidya, J. S. Witte, J. Yao, X. Zhu, R. G. Ziegler, A. B. Zonderman, A. Adeyemo, S. Ambs, M. Cushman, J. D. Faul, H. Hakonarson, A. M. Levin, K. L. Nathanson, E. B. Ware, D. R. Weir, W. Zhao, D. Zhi, D. K. Arnett, S. F. A. Grant, S. L. R. Kardia, O. I. Oloapde, D. C. Rao, C. N. Rotimi, M. M. Sale, L. K. Williams, B. S. Zemel, D. M. Becker, I. B. Borecki, M. K. Evans, T. B. Harris, J. N. Hirschhorn, Y. Li, S. R. Patel, B. M. Psaty, J. I. Rotter, J. G. Wilson, D. W. Bowden, L. A. Cupples, C. A. Haiman, R. J. F. Loos, K. E. North, Discovery and fine-mapping of adiposity loci using high density imputation of genome-wide association studies in individuals of African ancestry: African Ancestry Anthropometry Genetics Consortium. *PLoS Genet* **13**, e1006719 (2017).

43. G. K. Varshney, W. Pei, M. C. LaFave, J. Idol, L. Xu, V. Gallardo, B. Carrington, K. Bishop, M. Jones, M. Li, U. Harper, S. C. Huang, A. Prakash, W. Chen, R. Sood, J. Ledin, S. M. Burgess, High-throughput gene targeting and phenotyping in zebrafish using CRISPR/Cas9. *Genome Res.* **25**, 1030-1042 (2015).
44. T. R. Whitesell, R. M. Kennedy, A. D. Carter, E. L. Rollins, S. Georgijevic, M. M. Santoro, S. J. Childs, An alpha-smooth muscle actin (acta2/alphasma) zebrafish transgenic line marking vascular mural cells and visceral smooth muscle cells. *PLoS One* **9**, e90590 (2014).
45. M. K. K. Niazi, M. F. Nilsson, B. R. Danielsson, E. Bengtsson, Fully Automatic Heart Beat Rate Determination in Digital Video Recordings of Rat Embryos. (2009).
46. M. R. Lamprecht, D. M. Sabatini, A. E. Carpenter, CellProfiler: free, versatile software for automated biological image analysis. *Biotechniques* **42**, 71-75 (2007).
47. A. Louis, N. T. Nguyen, M. Muffato, H. Roest Crollius, Genomicus update 2015: KaryoView and MatrixView provide a genome-wide perspective to multispecies comparative genomics. *Nucleic Acids Res.* **43**, D682-689 (2015).
48. K. Labun, T. G. Montague, J. A. Gagnon, S. B. Thyme, E. Valen, CHOPCHOP v2: a web tool for the next generation of CRISPR genome engineering. *Nucleic Acids Res.* **44**, W272-276 (2016).
49. M. A. Moreno-Mateos, C. E. Vejnar, J. D. Beaudoin, J. P. Fernandez, E. K. Mis, M. K. Khokha, A. J. Giraldez, CRISPRscan: designing highly efficient sgRNAs for CRISPR-Cas9 targeting in vivo. *Nat Methods* **12**, 982-988 (2015).
50. L. E. Jao, S. R. Wente, W. Chen, Efficient multiplex biallelic zebrafish genome editing using a CRISPR nuclease system. *Proc. Natl. Acad. Sci. U. S. A.* **110**, 13904-13909 (2013).
51. J. Zhang, K. Kobert, T. Flouri, A. Stamatakis, PEAR: a fast and accurate Illumina Paired-End reAd mergeR. *Bioinformatics* **30**, 614-620 (2014).
52. W. R. Pearson, T. Wood, Z. Zhang, W. Miller, Comparison of DNA sequences with protein sequences. *Genomics* **46**, 24-36 (1997).

53. A. Dobin, C. A. Davis, F. Schlesinger, J. Drenkow, C. Zaleski, S. Jha, P. Batut, M. Chaisson, T. R. Gingeras, STAR: ultrafast universal RNA-seq aligner. *Bioinformatics* **29**, 15-21 (2013).
54. H. Li, B. Handsaker, A. Wysoker, T. Fennell, J. Ruan, N. Homer, G. Marth, G. Abecasis, R. Durbin, The Sequence Alignment/Map format and SAMtools. *Bioinformatics* **25**, 2078-2079 (2009).
55. W. McLaren, L. Gil, S. E. Hunt, H. S. Riat, G. R. Ritchie, A. Thormann, P. Flicek, F. Cunningham, The Ensembl Variant Effect Predictor. *Genome Biol.* **17**, 122 (2016).

Acknowledgments: The computations were performed on resources provided by SNIC through Uppsala Multidisciplinary Center for Advanced Computational Science (UPPMAX) under Project SNIC b2015283. The authors would like to acknowledge support from Science for Life Laboratory, the National Genomics Infrastructure (NGI) and UPPMAX for providing assistance in massive parallel sequencing and computational infrastructure. Support from the National Bioinformatics Infrastructure Sweden (NBIS) is also gratefully acknowledged. **Funding**: MdH is a fellow of the Swedish Heart-Lung Foundation (20170872) and is supported by project grants from the Swedish Heart-Lung Foundation (20140543, 20170678), the Swedish Research Council (2015-03657), and NIH/NIDDK (R01DK106236, R01DK107786, U01DK105554). **Author contributions**: BvdH and MdH conceived the study design. BvdH, AE, TK, SV and SJ performed the experiments. BvdH, AE, EM, OD and MdH conceived the sequencing quality control and variant calling pipeline. BvdH, AA, HLB and MdH performed the image quantification and statistical analysis. BvdH and MdH wrote the manuscript. All authors provided critical feedback to the manuscript. **Competing interests**: There are no competing interests. **Data and materials availability**: Supplemental videos have been deposited at https://www.dropbox.com/s/3dboz7nq3emkz6z/Supp_videos.zip?dl=0.

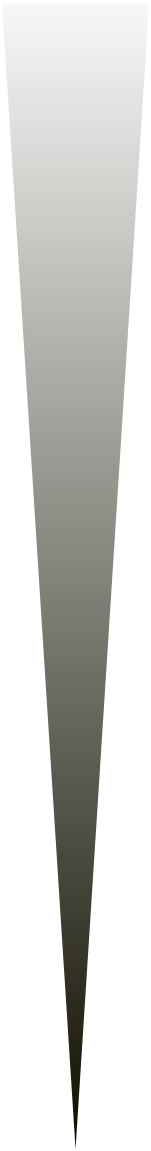

Fig. 1: Experimental pipeline describing the workflow from candidate gene selection to trait association. dpf = days post fertilization. VEP = Variant Effect Predictor.

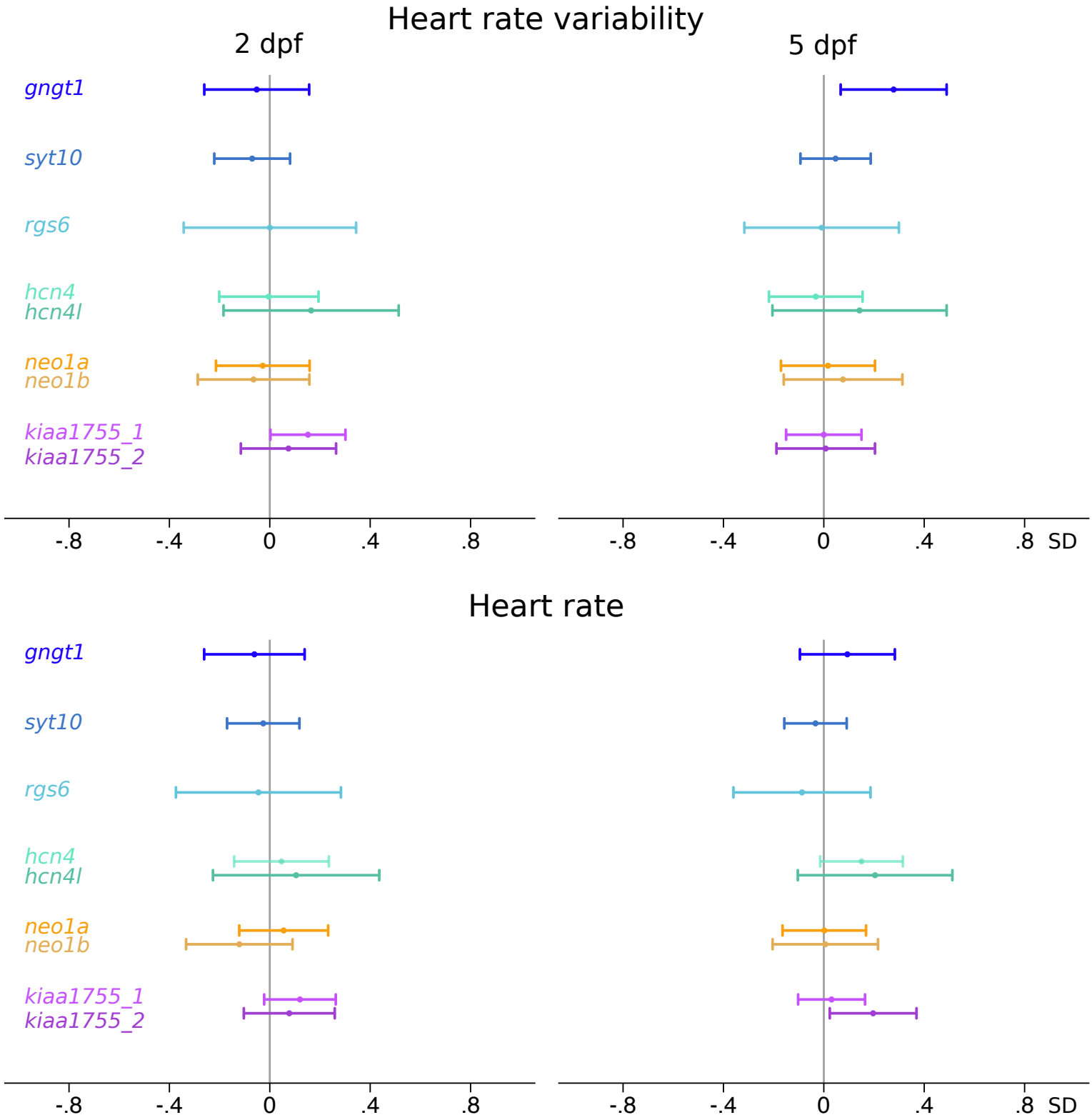

Fig. 2: Effect of mutations in candidate genes on heart rhythm and rate. Dots and whiskers show the effect size and its 95% confidence interval for each additional mutated allele, weighted by its predicted effect on protein function. Effects were adjusted for the number of mutated alleles in the other genes, as well as for heart rate or heart rate variability and time of day (fixed factor), with larvae nested in batches (random factor).
Genes are ordered by chromosomal position in humans.

Table 1: Selected candidate genes and their zebrafish orthologues in GWAS-identified heart rate variability associated loci

rsID	Chr	Human gene	ENSG	Zebrafish orthologue	ENSDARG
rs4262, rs180238	7	*GNG11*	ENSG00000127920	*gngt1*	ENSDARG00000035798
rs7980799, rs1351682, rs1384598	12	*SYT10*	ENSG00000110975	*syt10*	ENSDARG00000045750
rs4899412, rs2052015, rs2529471, rs36423	14	*RGS6*	ENSG00000182732	*rgs6*	ENSDARG00000015627
rs2680344	15	*HCN4*	ENSG00000138622	*hcn4*	ENSDARG00000061685
				hcn4l	ENSDARG00000074419
rs1812835	15	*NEO1*	ENSG00000067141	*neo1a*	ENSDARG00000102855
				neo1b	ENSDARG00000075100
rs6123471	20	*KIAA1755*	ENSG00000149633	*quo (kiaa1755_1)*	ENSDARG00000073684
				si:dkey-65j6.2 (kiaa1755_2)	ENSDARG00000103586

rsID refers to the lead SNP(s) of the GWAS-identified loci (Nolte et. al, 2017). Multiple independent SNPs per locus can be present. For simplicity, *quo* is referred to as *kiaa1755_1*, and *si:dkey-65j6.2* as *kiaa1755_2*.

Table 2: Descriptive information on HRV and heart rate at 2 and 5dpf

Age	Trait	Mean	SD	1st	Median	3rd
2	SDNN	19.52	12.60	9.84	17.39	26.55
	RMSSD	11.60	8.93	6.43	8.73	13.12
	HRV	15.56	10.04	8.74	12.96	19.65
	HR	208	24	192	207	225
5	SDNN	13.30	17.18	5.18	7.60	11.72
	RMSSD	13.05	18.26	5.93	7.48	12.01
	HRV	13.18	17.06	5.65	7.72	12.06
	HR	265	35	244	261	286

Information based on data from 279 embryos at 2 days post-fertilization (dpf) and 291 larvae at 5 dpf. HRV was calculated by averaging SDNN and RMSSD. HRV, SDNN and RMSSD are shown in ms, whereas HR is shown in beats per min. 1st and 3rd refers to the respective quartile. HRV: heart rate variability; SDNN: standard deviation of the normal-to-normal interval; RMSSD: root mean square of successive heart beat interval differences; HR: heart rate.

Supplementary Materials

Materials and methods

Candidate gene selection

Candidate genes in GWAS-identified loci for HRV were identified as described in detail in Nolte et al. (2017) (*4*). Of the 18 identified candidate genes, six were selected for experimental follow-up. This selection was based on overlap with findings from GWAS for heart rate (*KIAA1755*, *SYT10*, *HCN4*, *GNG11*) (*5*), as well as with results from eQTL analyses in sinoatrial node and brain (*RGS6*). Additional candidate genes from the same or nearby loci were also selected for experimental follow-up, i.e. *NEO1*, which resides next to *HCN4*. Zebrafish orthologues of the human genes were identified using Ensembl, as well as using a comprehensive synteny search using Genomicus (*47*) (table S1). Of the selected genes, *GNG11*, *SYT10* and *RGS6* have one orthologue in zebrafish, and *KIAA1755*, *HCN4* and *NEO1* each have two orthologues, resulting in a total of nine zebrafish orthologues for six human candidate genes (Table 1). For simplicity, the *KIAA1755* orthologues *quo* and *si:dkey-65j6.2* have been referred to as *kiaa1755_1* and *kiaa1755_2*.

Mutagenesis

All nine zebrafish genes were targeted together using a multiplexed CRISPR-Cas9 approach described recently (*16*). Briefly, guide-RNAs (gRNAs) were selected using ChopChop (*48*) and CRISPRscan (*49*) (table S1), based on their predicted efficiency, a moderate to high GC-content, location in an early exon, and absence of predicted off-target effects without mismatches. Oligonucleotides were designed as described (*16*), consisting of a T7 or SP6 promotor sequence (for gRNAs starting with 'GG' or 'GA', respectively), a gene-specific gRNA-target sequence, and an overlap sequence to a generic gRNA. The gene-specific oligonucleotides were annealed to a generic 80 bp long oligonucleotide at 98°C for 2 mins, 50°C for 10 mins, and 72°C for 10 mins. The products were checked for correct length on a 2% agarose gel. The oligonucleotides were subsequently transcribed *in vitro* using the manufacturer's instructions (TranscriptAid T7 high yield transcription kit / MEGAscript SP6 transcription kit, both ThermoFisher Scientific, Waltham, USA). The gRNAs were purified, after which the integrity of the purified gRNAs was examined on a 2% agarose gel. The zebrafish codon-optimized plasmid pT3TS-nls-zCas9-nls was used as a template to produce Cas9 mRNA (*50*). The plasmid was linearized with Xba1, and then purified using the Qiaprep Spin Miniprep kit (Qiagen, Hilden, Germany). The DNA was transcribed using the mMESSAGE mMACHINE T3 Transcription Kit (ThermoFisher Scientific, Waltham, USA), followed by LiCl precipitation. The quality of the RNA was confirmed on a 1% agarose gel.

Quality control of data

A series of quality control steps was performed to ensure only high-quality data was included in the genetic association analysis (fig. S1). First, graphs indicating that one or more true beats were missed by the script were removed from the analysis *a priori* (fig. S1). Second, larvae with any secondary phenotype (i.e. uncontrolled atrial contractions, sinoatrial pause or arrest, edema, abnormal morphology and/or reduced contractility) were excluded from the analyses for HRV and heart rate (primary analysis) (fig. S1). Third, genetic effects on these secondary traits were examined at 2dpf and 5dpf for traits with at least five cases (secondary analysis). Furthermore, embryos and larvae that showed a sinoatrial pause or arrest in between positioning and video acquisition, but not during the recording, were excluded from the analysis for sinoatrial pauses and arrests, since we cannot ascertain case status in the same rigorous manner for such samples, but they are not appropriate controls either.

Sample preparation for sequencing

After imaging at 5dpf, larvae were sacrificed by prolonged exposure to tricaine, and DNA was extracted by exposure to lysis buffer (10mM Tris-HCl pH8, 50mM KCl, 1mM EDTA, 0.3% Tween 20, 0.3% Igepal) and proteinase K (Roche Diagnostics, Mannheim, Germany) for 2 h at 55°C, followed by 10 min at 95°C to deactivate the proteinase K. Gene-specific primers amplifying gRNA-targeted regions between 150 and 300 bp were distilled from ChopChop (*48*), and Illumina adaptor-sequences were added. The first PCR was conducted by denaturation at 98°C for 30s; amplification for 35 cycles at 98°C for 10s, 62°C for 30s and 72°C for 30s; followed by a final extension at 72°C for 2 mins. Amplified PCR products were cleaned using magnetic beads (Mag-Bind PCR Clean-up Kit, Omega Bio-tek Inc. Norcross, GA). The purified products were used as a template for the second PCR, in which Illumina Nextera DNA library sequences were attached to allow multiplexed sequencing of all CRISPR-targeted sites across 384 larvae in a single lane. The second PCR amplification was performed by denaturation at 98°C for 30s; amplification for 25 cycles at 98°C for 10s, 66°C for 30s and 72°C for 30s; followed by a final extension at 72°C for 2 mins. Products were then purified using magnetic beads. All liquid handling was performed using a Hamilton Nimbus robot equipped with a 96-head (Hamilton robotics, Kista, Sweden). Samples were pooled and sequenced in a single lane on a MiSeq (300 bp paired-end, Illumina Inc., San Diego, CA) at the National Genomics Infrastructure, Sweden.

Processing of sequencing data

A custom-written bioinformatics pipeline was developed in collaboration with the National Bioinformatics Infrastructure Sweden to prepare .fastq files for analysis. First, a custom-written script was used to de-multiplex the .fastq files by gene and well. PEAR (*51*) was then used to merge paired-end reads, followed by removal of

low-quality reads using FastX (*52*). The reads were then mapped to the wildtype zebrafish genome (Zv11) using STAR (*53*). Next, we converted files from .sam to .bam format using samtools (*54*), after which variants - mostly indels and SNVs - were called allele specifically using a custom-written variant calling algorithm in R (Danio rerio Identification of Variants by Haplotype - DIVaH). All unique variants (table S2) located within ±30bps of the CRISPR-targeted sites that were identified across the two alleles were subsequently pooled, and used for functional annotation using Ensembl's VEP (*55*). Transcript-specific dosage scores were then calculated by retaining the variant with the highest predicted impact on protein function, and assigning it a score of 0 (no effect), 0.2 (modifier variant), 0.33 (low), 0.66 (moderate) or 1 (high). Transcript-specific dosage scores were subsequently calculated by summing the allele-specific scores at each embryo and target site. Since all transcripts within a target site were affected virtually identically, we only used the main transcript of each target site for the genetic association analysis.

Most larvae had successfully called sequences in all nine CRISPR-targeted sites (n=288, 75%). Of the 96 remaining embryos, 83 larvae (22%) had a missing sequence at one target site, and 11 larvae (3%) had two missing sequences. The remaining two larvae (0.5%) had three and four missing sequences, respectively. These two larvae have been excluded from the genetic association analysis. For the remaining larvae, the mean dosage of the transcript was imputed for missing calls. At a gene-level, a median of 380 larvae were successfully sequenced and called across all nine main transcripts, and all but one gene had successfully called mutations in ≥375 larvae. For *neo1b*, calling failed in 79 larvae (table S3). The imputed mean dosage for the main transcript of *neo1b* was still included in the genetic association analysis, since the mutant allele frequency in successfully called larvae was high (i.e. 0.798), and using an imputed dosage was anticipated to influence the results less than to discard the gene while it had been targeted. However, the results for *neo1b* should be interpreted in light of its call rate. The mutant allele frequency was low for *hcn4*, *hcn4l* and *rgs6*. For the remaining orthologues we had at least 10 wildtype and 10 compound heterozygous mutants.

Interrogating the druggability of the candidate genes

All human orthologues of the zebrafish genes that we found an effect for were interrogated in the drug-gene interaction database (DGIdb) v3.0.2 (*18*). The human interaction partners of the candidates (table S8) were distilled from STRING v10.5 (*21*) and GeneMania (*20*). The GeneMania search was limited to physical interactions and pathway data.

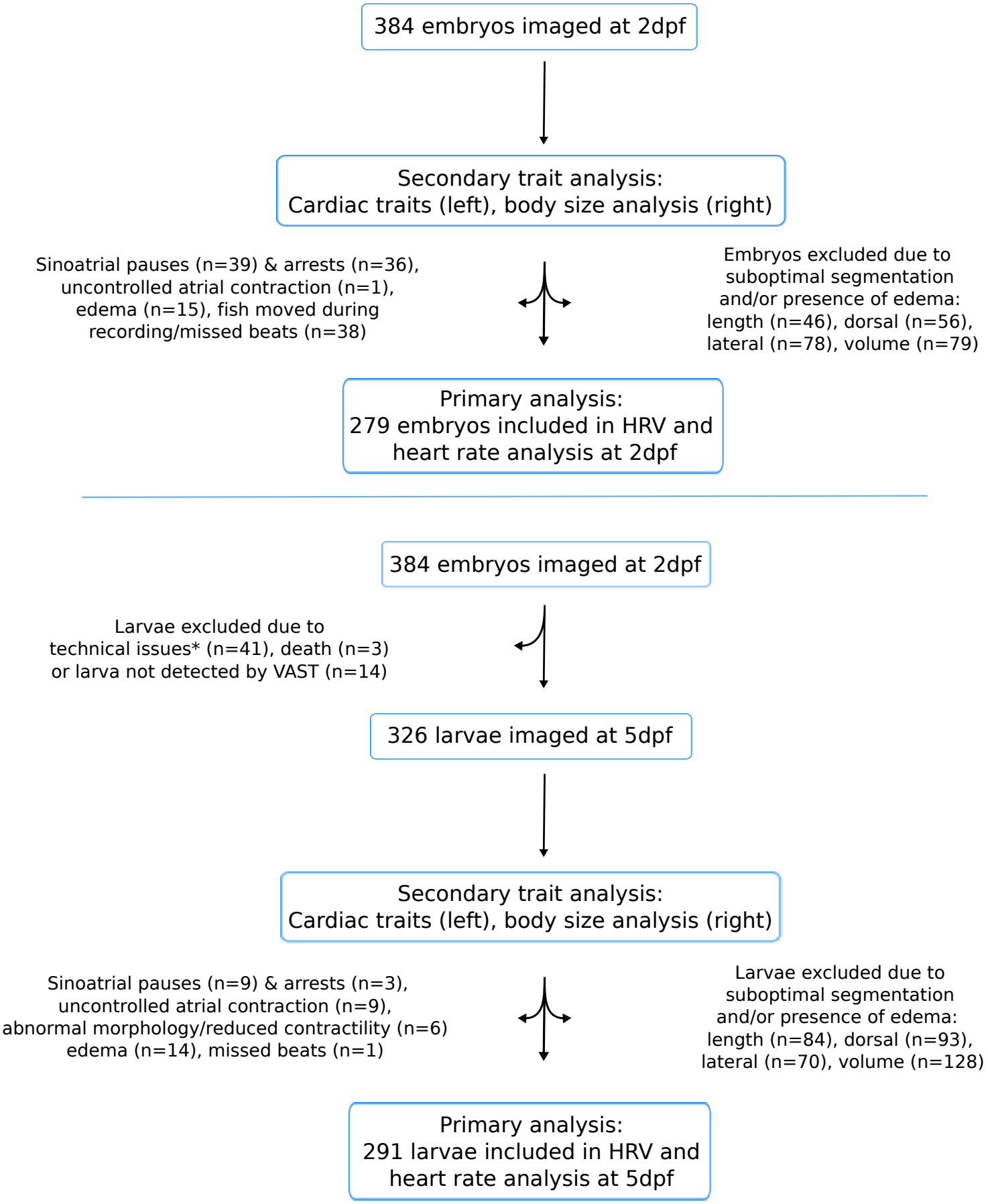

Fig. S1: Flow chart showing the number of included larvae in the analysis and reasons for exclusions. Embryos/larvae can show more than one phenotype. *Technical issues refers to not being able to image due to microscope complications. VAST: Vertebrate automated screening technology.

Supplementary Table 1: Overview of zebrafish orthologues and designed gRNAs

Zebrafish orthologue	ENSDARG	Conservation Zebrafish - Human	Conservation Zebrafish - Spotted gar	Main transcript	Target sequence gRNA	Exon target (transcript name)	CRISPRscan rank	ChopChop rank	Activity test rank	Predicted off-targets	Nr of mismatches	Genomic location of potential off-target 1	ENSDARG (gene-ID) of potential off-target 1, Feature	ENSG (gene-ID) of potential off-target 1	Genomic location of potential off-target 2	ENSDARG (gene-ID) of potential off-target 2, Feature	ENSG (gene-ID) of potential off-target 2	Primer forward	Primer reverse	Amplicon size
gngt1	ENSDARG00000035798	17	21	ENSDART00000051950	gGACCTGGATAAGGCGAAGA	2/3 (gngt1-001); 1/2 (gngt1-002)	62	4/13 (yellow)	moderate	1	3	chr25:17488676	ENSDARG00000051959 (zgc:66449), intron (3/6), intron (4/4)	no human orthologue				GTCCATTTTTCCAGAGTGGAGAC	gCCCATAACACAATTGCTTACC	207
syt10	ENSDARG00000045750	0	1	ENSDART00000136049	GGCTGATGCCGTCCTCTGTG	1/7 (syt10-001); 1/7 (syt10-201)	36	6/129 (green)	low	0								TAGGATATGGACTTGGACGCAT	TTACCTGGTATGTTGCTCTCCA	227
rgs6	ENSDARG00000015627	9	20	ENSDART00000135513	GGCCTCTCAGGACCAAGG	1/17 (rgs6-201); 2/18 (rgs6-001)	62	1/107 (green)	low	0								AAGGCTAATTCATTGTCTGGGA	GCATGTCAAATGTAAAGGCAAA	169
hcn4	ENSDARG00000061685	6	3	ENSDART00000136140	GGAGAGCCCTCCTGGAGCCG	1/8 (hcn4-001)	59	11/280 (green)	high	2	3/3	chr21:45844184	ENSDARG00000103825 (galnt10), exon (1/3)	ENSG00000164574 (GALNT10)	chrUn_KN150614v1:3424	ENSDARG00000100453 (*galnt10*), exon (6/8)	ENSG00000164574 (GALNT10)	CCTTTCGTCCATCACCAGTC	CCGCTTGATAATACCTCTCGTC	230
hcn4l	ENSDARG00000074419	3	3	ENSDART00000088249	gGCCTGGATAGTGTTTAACG	2/8 (hcn4l-201); 1/7 (hcn4l-001)	/	2/191 (green)	low	0								TTACTGGGACCTGATCATGCTT	AAGATGTAATCCACAGGGCATGG	235
neo1a	ENSDARG00000102855	1	5	ENSDART00000158160	GGAGCCGTCGGATACACTAG	1/4 (neo1a-001); 2/29 (neo1a-201); 2/30 (neo1a-202)	48	2/55 (green)	very high	0								TTCTGTGTCTCCACAGGATCAG	CCTCATCGGGTTTATTGTGTTT	215
neo1b	ENSDARG00000075100	2	6	ENSDART00000115280	GGACAGAGATGCTCGGCCTG	3/29 (neo1b-201)	58	18/354 (green)	very high	0								CAGCTCTCTCTCTCATTGGCTT	TATGGTGCAACGGTAGAGTCC	206
quo (kiaa1755_1)	ENSDARG00000073684	2	5	ENSDART00000109679	GGAGATCCGGTTGCCCTGTG	2/22 (quo-001); 3/23 (quo-201)	83	12/331 (green)	very high	0								ATGACCGTAAGTCAAGGGAAAA	TGAATCTTGTCTAATGGCGTTG	153
si:dkey-65j6.2 (kiaa1755_2)	ENSDARG00000103586	3	5	ENSDART00000158832	GGACGGTTTGGCTCCAGCAG	1/23 (si:dkey-65j6.2-201); 3/25 (si:dkey-65j6.2-001)	59	14/303 (green)	very high	2	3/3	chr15:32969618	ENSDARG00000104664 (dclk1b), exon (3/16), exon (4/17)	ENSG00000133083 (DCLK1)	chr22:28819880	ENSDARG00000071083 (si:dkeyp-34c12.2), Intron (7/7), Exon (8/9)	no human orthologue	AGCCATTACACCCAAAGAAAAA	GGGAATCATTTCGAAGTAGCTG	152

Table showing zebrafish genes, main transcript used for the analysis and gRNAs; rsID refers to the lead SNP(s) of the GWAS-identified loci (Nalbe et. al, 2017), multiple independent SNPs per locus can be present; For simplicity, *quo* is referred to as *kiaa1755_1*, and *si:dkey-65j6.2* as *kiaa1755_2*; Conservation refers to the number of genes that are preserved in the same locus across species according to Genomicus; A small "g" in the gRNA target sequence indicates a manually introduced nu

Supplementary Table 2: Unique variants and affected transcripts

Orthologue	Chr	Affected gene	ENSDARG	Affected transcripts	Start (bp)	End (bp)	Mutation	Annotation	Base pair change	VEP impact	Nr affected alleles
					40 856 894	40 856 894	A/-	frameshift variant	-1	High	69
					40 856 897	40 856 896	-/TAAC	stop gained,frameshift variant	4	High	2
					40 856 897	40 856 899	ATG/CCA	missense variant	0	Moderate	2
		gngt1	ENSDARG00000035798	ENSDART00000051950 ENSDART00000139083	40 856 888	40 856 893	AAGGCG/-	inframe deletion	-6	Moderate	75
					40 856 893	40 856 895	GAA/-	inframe deletion	-3	Moderate	3
					40 856 895	40 856 897	AGA/TTT	missense variant	0	Moderate	69
					40 856 895	40 856 895	A/T	missense variant	0	Moderate	3
					40 856 888	40 856 893	AAGGCG/-	upstream gene variant	-6	Modifier	75
					40 856 894	40 856 894	A/-	upstream gene variant	-1	Modifier	69
					40 856 895	40 856 895	A/T	upstream gene variant	0	Modifier	3
gngt1	19	*tfpi2*	ENSDARG00000061351	ENSDART00000087421	40 856 893	40 856 895	GAA/-	upstream gene variant	-3	Modifier	3
					40 856 895	40 856 897	AGA/TTT	upstream gene variant	0	Modifier	69
					40 856 897	40 856 896	-/TAAC	upstream gene variant	4	Modifier	2
					40 856 897	40 856 899	ATG/CCA	upstream gene variant	0	Modifier	2
					40 856 897	40 856 896	-/TAAC	upstream gene variant	4	Modifier	2
					40 856 888	40 856 893	AAGGCG/-	upstream gene variant	-6	Modifier	75
					40 856 895	40 856 897	AGA/TTT	upstream gene variant	0	Modifier	69
		zgc:85777	ENSDARG00000027009	ENSDART00000126470	40 856 897	40 856 899	ATG/CCA	upstream gene variant	0	Modifier	2
					40 856 895	40 856 895	A/T	upstream gene variant	0	Modifier	3
					40 856 894	40 856 894	A/-	upstream gene variant	-1	Modifier	69
					40 856 893	40 856 895	GAA/-	upstream gene variant	-3	Modifier	3
					10 888 946	10 888 950	GCACA/-	frameshift variant	-5	High	3
					10 888 950	10 888 949	-/A	frameshift variant	1	High	44
					10 888 950	10 888 949	-/GGGAATGG	frameshift variant	8	High	42
					10 888 949	10 888 958	CAGAGGACGG/-	frameshift variant	-10	High	4
					10 888 946	10 888 952	GCACAGA/-	frameshift variant	-7	High	15
					10 888 946	10 888 953	GCACAGAG/-	frameshift variant	-8	High	40
					10 888 948	10 888 954	ACAGAGG/-	frameshift variant	-7	High	11
					10 888 951	10 888 951	G/T	stop gained	0	High	42
syt10	4	*syt10*	ENSDARG00000045750	ENSDART00000136049	10 888 952	10 888 951	-/CAT	stop gained,protein altering variant	3	High	11
					10 888 952	10 888 952	A/-	frameshift variant	-1	High	42
					10 888 959	10 888 960	CA/TG	missense variant	0	Moderate	4
					10 888 948	10 888 948	A/C	missense variant	0	Moderate	4
					10 888 945	10 888 944	-/CAGCTGATG	inframe insertion	9	Moderate	42
					10 888 952	10 888 953	AG/CA	missense variant	0	Moderate	11
					10 888 933	10 888 953	GACATGAATGTCCGCACAGAG/-	inframe deletion	-21	Moderate	19
					10 888 947	10 888 947	C/T	synonymous variant	0	Low	42
					10 888 950	10 888 950	A/G	synonymous variant	0	Low	11
					10 888 944	10 888 944	C/A	synonymous variant	0	Low	42

Continued **Supplementary Table 2**

Orthologue	Chr	Affected gene	ENSDARG	Affected transcripts	Start (bp)	End (bp)	Mutation	Annotation	Base pair change	VEP impact	Nr affected alleles
					28 638 820	28 638 820	C/-	frameshift variant	-1	High	24
					28 638 820	28 638 821	CC/-	frameshift variant	-2	High	7
		rgs6	ENSDARG00000015627	ENSDART00000135513	28 638 824	28 638 824	G/A	stop gained	0	High	4
				ENSDART00000184779	28 638 837	28 638 836	-/CTGAGCCATG	frameshift variant	10	High	4
					28 638 820	28 638 822	CCT/-	inframe deletion	-3	Moderate	4
rgs6	20				28 638 811	28 638 822	CCCACCGCACCT/-	inframe deletion	-12	Moderate	1
					28 638 811	28 638 822	CCCACCGCACCT/-	upstream gene variant	-12	Modifier	1
					28 638 820	28 638 821	CC/-	upstream gene variant	-2	Modifier	7
		BX569801.2	ENSDARG00000096790	ENSDART00000153045	28 638 820	28 638 820	C/-	upstream gene variant	-1	Modifier	24
					28 638 820	28 638 822	CCT/-	upstream gene variant	-3	Modifier	4
					28 638 824	28 638 824	G/A	upstream gene variant	0	Modifier	4
					28 638 837	28 638 836	-/CTGAGCCATG	upstream gene variant	10	Modifier	4
				ENSDART00000136140	1 143 622	1 143 621	-/CTCCCCCGCCG	frameshift variant	11	High	2
					1 143 665	1 143 668	GGCT/-	frameshift variant	-4	High	9
					1 143 663	1 143 663	G/A	stop gained	0	High	9
					1 143 668	1 143 667	-/GCCA	frameshift variant	4	High	48
					1 143 666	1 143 665	-/CCGCCAC	frameshift variant	7	High	16
					1 143 667	1 143 667	C/-	frameshift variant	-1	High	2
					1 143 667	1 143 666	-/CTCTC	frameshift variant	5	High	15
					1 143 659	1 143 666	ACCCGCGG/-	frameshift variant	-8	High	13
		hcn4	ENSDARG00000061685	ENSDART00000136140 ENSDART00000189186	1 143 665	1 143 665	G/-	frameshift variant	-1	High	11
					1 143 668	1 143 668	T/C	missense variant	0	Moderate	48
					1 143 665	1 143 666	GG/CA	missense variant	0	Moderate	2
					1 143 674	1 143 673	-/AGCTCC	inframe insertion	6	Moderate	15
					1 143 666	1 143 668	GCT/-	inframe deletion	-3	Moderate	1
					1 143 660	1 143 660	C/T	missense variant	0	Moderate	16
					1 143 667	1 143 666	-/GCC	inframe insertion	3	Moderate	2
					1 143 666	1 143 666	G/C	missense variant	0	Moderate	75
hcn4	18			ENSDART00000189186	1 143 622	1 143 621	-/CTCCCCCGCCG	intron variant	11	Modifier	2
					1 143 663	1 143 663	G/A	upstream gene variant	0	Modifier	9
					1 143 667	1 143 666	-/GCC	upstream gene variant	3	Modifier	2
					1 143 622	1 143 621	-/CTCCCCCGCCG	upstream gene variant	11	Modifier	2
					1 143 660	1 143 660	C/T	upstream gene variant	0	Modifier	16
					1 143 668	1 143 668	T/C	upstream gene variant	0	Modifier	48
					1 143 665	1 143 668	GGCT/-	upstream gene variant	-4	Modifier	9
					1 143 666	1 143 665	-/CCGCCAC	upstream gene variant	7	Modifier	16
					1 143 666	1 143 666	G/C	upstream gene variant	0	Modifier	75
		rec114	ENSDARG00000069781	ENSDART00000135055	1 143 674	1 143 673	-/AGCTCC	upstream gene variant	6	Modifier	15
					1 143 667	1 143 666	-/CTCTC	upstream gene variant	5	Modifier	15
					1 143 667	1 143 667	C/-	upstream gene variant	-1	Modifier	2
					1 143 668	1 143 667	-/GCCA	upstream gene variant	4	Modifier	48
					1 143 665	1 143 666	GG/CA	upstream gene variant	0	Modifier	2
					1 143 659	1 143 666	ACCCGCGG/-	upstream gene variant	-8	Modifier	13
					1 143 666	1 143 668	GCT/-	upstream gene variant	-3	Modifier	1
					1 143 665	1 143 665	G/-	upstream gene variant	-1	Modifier	11

Continued **Supplementary Table 2**

Orthologue	Chr	Affected gene	ENSDARG	Affected transcripts	Start (bp)	End (bp)	Mutation	Annotation	Base pair change	VEP impact	Nr affected alleles
hcn4l	25	*hcn4l*	ENSDARG00000074419	ENSDART00000088249 ENSDART00000148940	29 273 091	29 273 090	-/T	frameshift variant	1	High	4
					29 273 086	29 273 101	CCACGTTAAACACTAT/-	frameshift variant	-16	High	9
					29 273 092	29 273 093	TA/-	frameshift variant	-2	High	18
		RF00001	ENSDARG00000081202	ENSDART00000115672	29 273 091	29 273 090	-/T	downstream gene variant	1	Modifier	4
					29 273 092	29 273 093	TA/-	downstream gene variant	-2	Modifier	18
					29 273 086	29 273 101	CCACGTTAAACACTAT/-	downstream gene variant	-16	Modifier	9
neo1a	7	*neo1a*	ENSDARG00000102855	ENSDART00000158160 ENSDART00000163261 ENSDART00000164768 ENSDART00000181629	53 879 242	53 879 248	ATACACT/-	frameshift variant	-7	High	5
					53 879 243	53 879 247	TACAC/-	frameshift variant	-5	High	17
					53 879 262	53 879 265	GCGC/-	frameshift variant	-4	High	5
					53 879 235	53 879 265	CCGTCGGATACACTAGCGGTGCGAGGAGCGC/-	frameshift variant	-31	High	57
					53 879 247	53 879 246	-/GCGGTGCGAGGAGT	frameshift variant	14	High	1
					53 879 247	53 879 246	-/TCCAT	frameshift variant	5	High	14
					53 879 228	53 879 244	CACGGAGCCGTCGGATA/-	frameshift variant	-17	High	1
					53 879 231	53 879 258	GGAGCCGTCGGATACACTAGCGGTGCGA/-	frameshift variant	-28	High	11
					53 879 240	53 879 246	GGATACA/-	frameshift variant	-7	High	2
					53 879 243	53 879 268	TACACTAGCGGTGCGAGGAGCGCCAG/-	frameshift variant	-26	High	16
					53 879 247	53 879 250	CTAG/-	frameshift variant	-4	High	82
					53 879 237	53 879 267	GTCGGATACACTAGCGGTGCGAGGAGCGCCA/-	frameshift variant	-31	High	9
					53 879 250	53 879 254	GCGGT/-	frameshift variant	-5	High	2
					53 879 263	53 879 262	-/CGCCAGTTCT	frameshift variant	10	High	89
					53 879 237	53 879 252	GTCGGATACACTAGCG/-	frameshift variant	-16	High	157
					53 879 245	53 879 255	CACTAGCGGTG/-	frameshift variant	-11	High	20
					53 879 248	53 879 258	TAGCGGTGCGA/-	frameshift variant	-11	High	5
					53 879 247	53 879 248	CT/TC	missense variant	0	Moderate	14
					53 879 248	53 879 248	T/C	missense variant	0	Moderate	10
					53 879 266	53 879 266	C/T	missense variant	0	Moderate	5
					53 879 248	53 879 247	-/GGTGCG	protein altering variant	6	Moderate	6
					53 879 247	53 879 252	CTAGCG/-	inframe deletion	-6	Moderate	10
					53 879 249	53 879 260	AGCGGTGCGAGG/-	inframe deletion	-12	Moderate	5
					53 879 245	53 879 246	CA/GT	missense variant	0	Moderate	5
					53 879 247	53 879 255	CTAGCGGTG/-	inframe deletion	-9	Moderate	69
					53 879 244	53 879 245	AC/GT	missense variant	0	Moderate	1
					53 879 239	53 879 250	CGGATACACTAG/-	inframe deletion	-12	Moderate	66
					53 879 253	53 879 254	GT/AA	missense variant	0	Moderate	10
					53 879 246	53 879 248	ACT/-	inframe deletion	-3	Moderate	20
					53 879 248	53 879 248	T/G	missense variant	0	Moderate	6
					53 879 247	53 879 247	C/G	missense variant	0	Moderate	1
					53 879 249	53 879 249	A/G	synonymous variant	0	Low	2

Continued **Supplementary Table 2**

Orthologue	Chr	Affected gene	ENSDARG	Affected transcripts	Start (bp)	End (bp)	Mutation	Annotation	Base pair change	VEP impact	Nr affected alleles
					2 899 716	2 899 722	GGCCTGT/-	frameshift variant	-7	High	7
					2 899 719	2 899 718	-/AG	frameshift variant	2	High	1
					2 899 719	2 899 718	-/TCGG	frameshift variant	4	High	50
					2 899 715	2 899 731	CGGCCTGTGGAGCTGGA/-	frameshift variant	-17	High	6
					2 899 710	2 899 728	ATGCTCGGCCTGTGGAGCT/-	frameshift variant	-19	High	7
					2 899 722	2 899 721	-/GGTC	frameshift variant	4	High	15
					2 899 718	2 899 718	C/-	frameshift variant	-1	High	58
neo1b	25	*neo1b*	ENSDARG00000075100	ENSDART00000115280	2 899 707	2 899 728	GAGATGCTCGGCCTGTGGAGCT/-	frameshift variant	-22	High	2
					2 899 715	2 899 718	CGGC/-	frameshift variant	-4	High	13
					2 899 719	2 899 718	-/AGCAGGGT	frameshift variant	8	High	15
					2 899 713	2 899 718	CTCGGC/-	inframe deletion	-6	Moderate	120
					2 899 740	2 899 740	T/A	missense variant	0	Moderate	7
					2 899 698	2 899 698	G/A	missense variant	0	Moderate	2
					2 899 734	2 899 737	GCAG/TTCA	missense variant	0	Moderate	7
					2 899 719	2 899 724	CTGTGG/-	inframe deletion	-6	Moderate	50
					2 899 711	2 899 719	TGCTCGGCC/-	inframe deletion	-9	Moderate	19

Continued **Supplementary Table 2**

Orthologue	Chr	Affected gene	ENSDARG	Affected transcripts	Start (bp)	End (bp)	Mutation	Annotation	Base pair change	VEP impact	Nr affected alleles
					2 051 712	2 051 728	CAGGGCAACCGGATCTC/-	frameshift variant	-17	High	23
					2 051 712	2 051 711	-/CCGG	frameshift variant	4	High	1
					2 051 710	2 051 716	CACAGGG/-	frameshift variant	-7	High	53
					2 051 713	2 051 712	-/TTG	stop gained,inframe insertion	3	High	70
					2 051 714	2 051 714	G/-	frameshift variant	-1	High	22
					2 051 719	2 051 723	ACCGG/-	frameshift variant	-5	High	17
					2 051 713	2 051 712	-/A	frameshift variant	1	High	19
					2 051 712	2 051 711	-/ACCGGACT	frameshift variant	8	High	7
					2 051 709	2 051 715	TCACAGG/-	frameshift variant	-7	High	9
					2 051 713	2 051 712	-/G	frameshift variant	1	High	15
					2 051 699	2 051 699	A/T	stop gained	0	High	10
					2 051 713	2 051 716	AGGG/-	frameshift variant	-4	High	4
					2 051 710	2 051 719	CACAGGGCAA/-	frameshift variant	-10	High	51
					2 051 712	2 051 716	CAGGG/-	frameshift variant	-5	High	14
					2 051 703	2 051 716	CATTCCTCACAGGG/-	frameshift variant	-14	High	61
				ENSDART00000109679	2 051 715	2 051 714	-/C	frameshift variant	1	High	22
				ENSDART00000153568	2 051 715	2 051 715	G/C	missense variant	0	Moderate	22
kiaa1755_1	6	*kiaa1755_1*	ENSDARG00000073684	ENSDART00000187502 ENSDART00000187544 ENSDART00000191165	2 051 654	2 051 734	ATGACCCAACTTATCACAAGCATGGTCCAAGCAA GACAGCATCACAAGTCATTCCTCACAGGGCAACC GGATCTCCCTCAG/-	inframe deletion	-81	Moderate	13
					2 051 724	2 051 724	A/T	missense variant	0	Moderate	17
					2 051 714	2 051 714	G/A	missense variant	0	Moderate	40
					2 051 736	2 051 736	C/A	missense variant	0	Moderate	13
					2 051 714	2 051 714	G/C	missense variant	0	Moderate	15
					2 051 706	2 051 708	TCC/-	inframe deletion	-3	Moderate	17
					2 051 714	2 051 713	-/ACC	inframe insertion	3	Moderate	51
					2 051 713	2 051 714	AG/TA	missense variant	0	Moderate	70
					2 051 712	2 051 714	CAG/ACC	missense variant	0	Moderate	9
					2 051 719	2 051 720	AC/TT	missense variant	0	Moderate	1
					2 051 701	2 051 715	GTCATTCCTCACAGG/-	inframe deletion	-15	Moderate	10
					2 051 712	2 051 712	C/T	missense variant	0	Moderate	15
					2 051 716	2 051 716	G/A	synonymous variant	0	Low	10
					2 051 716	2 051 716	G/T	synonymous variant	0	Low	18
					2 051 713	2 051 713	A/C	synonymous variant	0	Low	22

Continued **Supplementary Table 2**

Orthologue	Chr	Affected gene	ENSDARG	Affected transcripts	Start (bp)	End (bp)	Mutation	Annotation	Base pair change	VEP impact	Nr affected alleles
					43 213 137	43 213 153	GGTTTGGCTCCAGCAGT/-	frameshift variant	-17	High	15
					43 213 140	43 213 147	TTGGCTCC/-	frameshift variant	-8	High	18
					43 213 159	43 213 160	GC/-	frameshift variant	-2	High	3
					43 213 136	43 213 149	CGGTTTGGCTCCAG/-	frameshift variant	-14	High	21
					43 213 145	43 213 149	TCCAG/-	frameshift variant	-5	High	9
					43 213 142	43 213 157	GGCTCCAGCAGTGGTC/-	frameshift variant	-16	High	3
					43 213 136	43 213 164	CGGTTTGGCTCCAGCAGTGGTCGGCACAT/-	frameshift variant	-29	High	50
					43 213 135	43 213 160	ACGGTTTGGCTCCAGCAGTGGTCGGC/-	frameshift variant	-26	High	1
					43 213 138	43 213 168	GTTTGGCTCCAGCAGTGGTCGGCACATCAGA/-	frameshift variant	-31	High	3
					43 213 146	43 213 161	CCAGCAGTGGTCGGCA/-	frameshift variant	-16	High	34
					43 213 146	43 213 146	C/-	frameshift variant	-1	High	41
					43 213 155	43 213 154	-/AAACACAGAGA	frameshift variant	11	High	41
					43 213 142	43 213 141	-/AAAAATAA	frameshift variant	8	High	7
					43 213 143	43 213 153	GCTCCAGCAGT/-	frameshift variant	-11	High	13
					43 213 146	43 213 150	CCAGC/-	frameshift variant	-5	High	7
				ENSDART00000158832	43 213 144	43 213 144	C/-	frameshift variant	-1	High	1
				ENSDART00000164262	43 213 140	43 213 151	TTGGCTCCAGCA/-	inframe deletion	-12	Moderate	7
kiaa1755_2	23	*kiaa1755_2*	ENSDARG00000103586	ENSDART00000186065	43 213 133	43 213 153	GGACGGTTTGGCTCCAGCAGT/-	inframe deletion	-21	Moderate	62
				ENSDART00000190315	43 213 136	43 213 156	CGGTTTGGCTCCAGCAGTGGT/-	inframe deletion	-21	Moderate	101
				ENSDART00000193300	43 213 153	43 213 153	T/A	missense variant	0	Moderate	41
					43 213 152	43 213 152	G/A	missense variant	0	Moderate	3
					43 213 149	43 213 149	G/T	missense variant	0	Moderate	41
					43 213 138	43 213 138	G/A	missense variant	0	Moderate	4
					43 213 140	43 213 160	TTGGCTCCAGCAGTGGTCGGC/-	inframe deletion	-21	Moderate	12
					43 213 149	43 213 149	G/C	missense variant	0	Moderate	18
					43 213 141	43 213 152	TGGCTCCAGCAG/-	inframe deletion	-12	Moderate	32
					43 213 140	43 213 140	T/A	missense variant	0	Moderate	3
					43 213 139	43 213 143	TTTGG/CACAT	missense variant	0	Moderate	9
					43 213 149	43 213 149	G/A	missense variant	0	Moderate	1
					43 213 155	43 213 157	GTC/AAT	missense variant	0	Moderate	41
					43 213 143	43 213 157	GCTCCAGCAGTGGTC/-	inframe deletion	-15	Moderate	57
					43 213 147	43 213 147	C/G	missense variant	0	Moderate	1
					43 213 147	43 213 149	CAG/-	inframe deletion	-3	Moderate	69
					43 213 139	43 213 139	T/G	synonymous variant	0	Low	18

The predicted impact of unique CRISPR-Cas9 induced mutations on protein function was assessed using Ensembl's Variant Effect Predictor (VEP). An allele- and target-specific dosage score was subsequently calculated for each larva by weighting the mutation with the highest predicted impact by a factor 0.33, 0.66, or 1 for mutations with a low, moderate or high predicted impact, respectively. Modification of expression was only observed for transcripts of genes located near the targeted gene. Start and end coordinates are based on GRCz11. For simplicity, *kiaa1755_1* refers to *quo*, and *kiaa1755_2* to *si:dkey-65j6.2*.

Supplementary Table 3: Mutant allele frequencies

	Nr mutated alleles						Expected nr mutated alleles			
Gene	**0**	**1**	**2**	**Missing**	**Sample call rate**	**Mutant allele freq**	**0**	**1**	**2**	**P_{HWE}**
gngt1	234	132	12	4	0.990	0.206	238	124	16	2.70E-01
syt10	193	131	54	4	0.990	0.316	177	163	38	2.10E-04
rgs6	346	34	1	1	0.997	0.047	346	34	1	5.79E-01
hcn4	268	100	9	5	0.987	0.156	268	100	9	4.69E-01
hcn4l	351	29	1	1	0.997	0.041	351	30	1	1.00E+00
neo1a	20	113	241	8	0.979	0.795	16	122	237	1.16E-01
neo1b	15	19	271	77	0.798	0.920	2	45	258	2.12E-13
kiaa1755_1	55	42	283	2	0.995	0.800	15	122	243	3.33E-32
kiaa1755_2	24	60	295	3	0.992	0.858	8	93	279	5.65E-10

Number of larvae with 0, 1 and 2 mutated alleles, as well as the number of larvae with a missing call. *P*-value for a Hardy-Weinberg equilibrium (HWE) exact test, considering a ±30 bp window around the CRISPR targeted site as a single locus (*P*<2.9E-3 is significant after Bonferroni correction). Larvae with more than two missing genotypes were excluded from the statistical analysis (i.e. n_total=382). For simplicity, *kiaa1755_1* refers to *quo*, and *kiaa1755_2* to *si:dkey-65j6.2*.

Supplementary Table 4: Transcript-specific association analysis for dichotomous cardiac outcomes

	Sinoatrial pause							
	2dpf (n=323, 39 cases)				5dpf (n=318, 9 cases)			
Gene	**OR**	**LCI**	**UCI**	**P**	**OR**	**LCI**	**UCI**	**P**
gngt1	1.581	0.711	3.517	2.61E-01	0.123	0.009	1.649	1.13E-01
syt10	1.734	1.018	2.953	4.27E-02	0.732	0.241	2.221	5.81E-01
rgs6	2.209	0.862	5.666	9.90E-02	3.862	0.637	23.411	1.42E-01
hcn4	3.041	1.656	5.584	3.34E-04	1.209	0.359	4.072	7.59E-01
hcn4l	1.269	0.327	4.930	7.31E-01	3.112	0.328	29.534	3.23E-01
neo1a	0.936	0.465	1.881	8.52E-01	0.747	0.218	2.558	6.42E-01
neo1b	2.014	0.705	5.749	1.91E-01	0.379	0.081	1.785	2.20E-01
kiaa1755_1	0.749	0.426	1.318	3.16E-01	0.582	0.219	1.547	2.78E-01
kiaa1755_2	1.045	0.479	2.278	9.12E-01	8.170	1.077	61.988	4.22E-02
time of day	0.932	0.704	1.234	6.25E-01	1.079	0.583	1.998	8.09E-01
intercept	0.030	0.003	0.298	2.81E-03	0.017	0.000	0.830	4.00E-02

	Sinoatrial arrest			
	2dpf (n=321, 36 cases)			
Gene	**OR**	**LCI**	**UCI**	**P**
gngt1	1.586	0.707	3.556	2.63E-01
syt10	1.639	0.952	2.821	7.47E-02
rgs6	1.988	0.737	5.357	1.75E-01
hcn4	2.906	1.556	5.428	8.19E-04
hcn4l	1.267	0.331	4.852	7.30E-01
neo1a	1.016	0.491	2.101	9.67E-01
neo1b	1.590	0.549	4.605	3.93E-01
kiaa1755_1	0.823	0.458	1.480	5.16E-01
kiaa1755_2	1.143	0.507	2.578	7.47E-01
time of day	0.928	0.697	1.236	6.10E-01
intercept	0.030	0.003	0.303	3.02E-03

	Cardiac edema							
	2dpf (n=369, 15 cases)				5dpf (n=322, 14 cases)			
Gene	**OR**	**LCI**	**UCI**	**P**	**OR**	**LCI**	**UCI**	**P**
gngt1	1.518	0.489	4.706	4.70E-01	7.780	1.755	34.480	6.92E-03
syt10	0.584	0.226	1.509	2.67E-01	0.901	0.291	2.787	8.57E-01
rgs6	0.702	0.086	5.739	7.42E-01	2.730	0.456	16.336	2.71E-01
hcn4	0.546	0.146	2.043	3.68E-01	0.380	0.065	2.213	2.82E-01
hcn4l	0.800	0.111	5.770	8.25E-01	0.039	0.000	63.816	3.90E-01
neo1a	0.844	0.309	2.307	7.41E-01	0.253	0.080	0.796	1.88E-02
neo1b	1.154	0.328	4.064	8.23E-01	0.217	0.046	1.028	5.42E-02
kiaa1755_1	1.137	0.505	2.563	7.56E-01	2.126	0.604	7.486	2.40E-01
kiaa1755_2	1.317	0.430	4.032	6.29E-01	2.011	0.414	9.761	3.86E-01
time of day	0.963	0.633	1.465	8.59E-01	1.675	0.930	3.016	8.57E-02
intercept	0.036	0.002	0.697	2.78E-02	0.017	0.001	0.513	1.90E-02

Continued **Supplementary Table 4**

	Uncontrolled atrial contractions 5dpf (n=326, 9 cases)			
Gene	**OR**	**LCI**	**UCI**	**P**
gngt1	2.578	0.502	13.247	2.57E-01
syt10	0.343	0.065	1.813	2.08E-01
rgs6	1.313	0.138	12.517	8.13E-01
hcn4	1.310	0.339	5.064	6.96E-01
hcn4l	-	-	-	-
neo1a	0.294	0.085	1.012	5.23E-02
neo1b	0.988	0.203	4.810	9.88E-01
kiaa1755_1	0.644	0.230	1.802	4.02E-01
kiaa1755_2	2.107	0.352	12.615	4.14E-01
time of day	0.648	0.335	1.251	1.96E-01
intercept	0.245	0.004	14.946	5.03E-01

	Abnormal morphology and impaired contractility 5dpf (n=326, 6 cases)			
Gene	**OR**	**LCI**	**UCI**	**P**
gngt1	41.888	3.401	515.945	3.55E-03
syt10	0.929	0.206	4.187	9.23E-01
rgs6	-	-	-	-
hcn4	0.348	0.021	5.883	4.64E-01
hcn4l	-	-	-	-
neo1a	0.150	0.026	0.850	3.21E-02
neo1b	0.145	0.015	1.379	9.29E-02
kiaa1755_1	1.916	0.371	9.885	4.38E-01
kiaa1755_2	0.628	0.099	3.979	6.21E-01
time of day	1.317	0.582	2.977	5.09E-01
intercept	0.076	0.001	5.737	2.43E-01

Associations of cardiac outcomes with the number of mutated alleles across the nine orthologues, weighted by their predicted effect on protein function. At 2 and 5 days post fertilization (dpf), associations were analyzed using logistic regression for outcomes that were observed in at least five larvae. Associations were adjusted for time of day and for the weighted number of mutated alleles in the other genes as fixed factors. '-' indicates that parameters could not be estimated. For simplicity, *kiaa1755_1* refers to *quo*, and *kiaa1755_2* to *si:dkey-65j6.2*.

Supplementary Table 5: Transcript-specific association analysis for HRV and heart rate

				Heart rate variability				
Age	**n**	**Factor**	**Gene**	**Effect size**	**SE**	**LCI**	**UCI**	**P**
2	279	fixed effects	*gngt1*	-0.052	0.107	-0.261	0.157	6.25E-01
			syt10	-0.070	0.077	-0.221	0.081	3.62E-01
			rgs6	0.000	0.175	-0.343	0.344	9.98E-01
			hcn4	-0.004	0.101	-0.202	0.194	9.70E-01
			hcn4l	0.165	0.178	-0.184	0.514	3.55E-01
			neo1a	-0.028	0.095	-0.214	0.158	7.69E-01
			neo1b	-0.065	0.113	-0.287	0.158	5.68E-01
			kiaa1755_1	0.152	0.076	0.003	0.302	4.61E-02
			kiaa1755_2	0.074	0.097	-0.115	0.264	4.42E-01
			time of day	0.503	0.045	0.414	0.592	1.77E-28
			Heart rate (in SD)	-0.459	0.056	-0.570	-0.348	4.59E-16
			intercept	-1.614	0.300	-2.202	-1.026	7.54E-08
		random effects	variation by batch	0.340	0.113	0.177	0.652	-
			residual	0.765	0.033	0.704	0.832	-
5	291	fixed effects	*gngt1*	0.278	0.108	0.067	0.489	9.81E-03
			syt10	0.047	0.071	-0.093	0.187	5.12E-01
			rgs6	-0.009	0.157	-0.317	0.299	9.56E-01
			hcn4	-0.032	0.095	-0.219	0.154	7.35E-01
			hcn4l	0.142	0.177	-0.205	0.489	4.22E-01
			neo1a	0.017	0.096	-0.171	0.204	8.62E-01
			neo1b	0.077	0.121	-0.160	0.313	5.25E-01
			kiaa1755_1	0.000	0.077	-0.150	0.150	1.00E+00
			kiaa1755_2	0.008	0.100	-0.189	0.204	9.40E-01
			time of day	0.524	0.052	0.422	0.626	7.54E-24
			Heart rate (in SD)	-0.645	0.054	-0.751	-0.540	2.86E-33
			intercept	-1.893	0.383	-2.643	-1.142	7.67E-07
		random effects	variation by batch	0.540	0.185	0.276	1.056	-
			residual	0.769	0.032	0.708	0.834	-

				Heart rate				
Age	**n**	**Factor**	**Gene**	**Effect size**	**SE**	**LCI**	**UCI**	**P**
2	279	fixed effects	*gngt1*	-0.061	0.102	-0.261	0.139	5.48E-01
			syt10	-0.026	0.074	-0.170	0.118	7.22E-01
			rgs6	-0.045	0.168	-0.374	0.284	7.88E-01
			hcn4	0.047	0.096	-0.142	0.236	6.27E-01
			hcn4l	0.105	0.169	-0.226	0.436	5.35E-01
			neo1a	0.055	0.090	-0.122	0.233	5.39E-01
			neo1b	-0.121	0.108	-0.333	0.091	2.62E-01
			kiaa1755_1	0.120	0.073	-0.022	0.263	9.83E-02
			kiaa1755_2	0.078	0.092	-0.104	0.259	4.01E-01
			time of day	0.550	0.040	0.472	0.627	9.14E-44
			HRV (in SD)	-0.408	0.051	-0.508	-0.308	1.23E-15
			intercept	-1.770	0.258	-2.276	-1.264	7.14E-12
		random effects	variation by batch	0.185	0.077	0.082	0.420	-
			residual	0.734	0.031	0.675	0.798	-
5	291	fixed effects	*gngt1*	0.094	0.097	-0.095	0.283	3.31E-01
			syt10	-0.033	0.063	-0.157	0.091	6.02E-01
			rgs6	-0.087	0.139	-0.360	0.186	5.32E-01
			hcn4	0.150	0.084	-0.014	0.315	7.37E-02
			hcn4l	0.204	0.157	-0.104	0.512	1.94E-01
			neo1a	0.002	0.085	-0.165	0.168	9.82E-01
			neo1b	0.006	0.107	-0.204	0.216	9.57E-01
			kiaa1755_1	0.031	0.068	-0.102	0.164	6.50E-01
			kiaa1755_2	0.197	0.088	0.024	0.369	2.59E-02
			time of day	0.564	0.043	0.480	0.648	1.97E-39
			HRV (in SD)	-0.516	0.043	-0.599	-0.432	7.79E-34
			intercept	-2.137	0.375	-2.872	-1.402	1.20E-08
		random effects	variation by batch	0.619	0.204	0.324	1.181	-
			residual	0.682	0.029	0.629	0.740	-

Associations of heart rate variability (HRV) and heart rate (mutually adjusted) with the number of mutated alleles across the nine orthologues, weighted by their predicted effect on protein function. Associations were examined for the main transcript of each targeted zebrafish orthologue using hierarchical linear models (xtmixed in Stata), using inverse-normally transformed outcomes, so effect sizes and SEs can be interpreted as z-score units. Associations were adjusted for time of day and the weighted number of mutated alleles in the other genes as fixed factors, with larvae nested in batches (random factor). For simplicity, *kiaa1755_1* refers to *quo*, and *kiaa1755_2* to *si:dkey-65j6.2*.

Supplementary Table 6: Transcript-specific association analysis for heart rate variability and heart rate in larvae without a sinoatrial pause before or after the recording

				Heart rate variability				
Age	**n**	**Factor**	**Gene**	**Effect size**	**SE**	**LCI**	**UCI**	**P**
2	234	fixed effects	*gngt1*	-0.066	0.122	-0.306	0.173	5.88E-01
			syt10	-0.058	0.084	-0.223	0.107	4.91E-01
			rgs6	0.036	0.201	-0.358	0.429	8.60E-01
			hcn4	0.029	0.111	-0.189	0.247	7.95E-01
			hcn4l	0.171	0.206	-0.232	0.575	4.05E-01
			neo1a	-0.056	0.105	-0.263	0.151	5.95E-01
			neo1b	-0.094	0.125	-0.338	0.150	4.50E-01
			kiaa1755_1	0.180	0.082	0.019	0.340	2.81E-02
			kiaa1755_2	0.093	0.102	-0.107	0.292	3.64E-01
			time of day	0.555	0.050	0.456	0.654	4.10E-28
			Heart rate (in SD)	-0.534	0.063	-0.658	-0.411	1.81E-17
			intercept	-1.770	0.316	-2.388	-1.151	2.05E-08
		random effects	variation by batch	0.344	0.118	0.176	0.674	-
			residual	0.769	0.036	0.702	0.843	-
5	283	fixed effects	*gngt1*	0.264	0.106	0.056	0.472	1.27E-02
			syt10	-0.005	0.071	-0.144	0.134	9.42E-01
			rgs6	-0.025	0.157	-0.333	0.282	8.72E-01
			hcn4	-0.042	0.094	-0.226	0.142	6.56E-01
			hcn4l	0.135	0.173	-0.203	0.474	4.33E-01
			neo1a	-0.002	0.094	-0.185	0.182	9.86E-01
			neo1b	0.055	0.118	-0.176	0.286	6.41E-01
			kiaa1755_1	0.020	0.077	-0.131	0.170	7.99E-01
			kiaa1755_2	0.081	0.102	-0.119	0.281	4.28E-01
			time of day	0.534	0.051	0.434	0.633	8.87E-26
			Heart rate (in SD)	-0.623	0.053	-0.727	-0.519	5.00E-32
			intercept	-1.978	0.372	-2.707	-1.250	1.01E-07
		random effects	variation by batch	0.516	0.178	0.263	1.013	-
			residual	0.747	0.032	0.687	0.812	-

				Heart rate				
Age	**N**	**Factor**	**Gene**	**Effect size**	**SE**	**LCI**	**UCI**	**P**
2	234	fixed effects	*gngt1*	-0.008	0.112	-0.228	0.212	9.43E-01
			syt10	-0.012	0.077	-0.162	0.139	8.78E-01
			rgs6	-0.114	0.184	-0.474	0.245	5.33E-01
			hcn4	0.041	0.101	-0.157	0.240	6.82E-01
			hcn4l	0.048	0.187	-0.317	0.414	7.95E-01
			neo1a	0.050	0.095	-0.137	0.236	6.01E-01
			neo1b	-0.165	0.113	-0.386	0.057	1.45E-01
			kiaa1755_1	0.153	0.075	0.007	0.300	4.00E-02
			kiaa1755_2	0.113	0.093	-0.069	0.295	2.24E-01
			time of day	0.586	0.041	0.505	0.666	5.48E-46
			HRV (in SD)	-0.434	0.051	-0.535	-0.333	3.28E-17
			intercept	-1.890	0.256	-2.392	-1.388	1.60E-13
		random effects	variation by batch	0.171	0.077	0.071	0.414	-
			residual	0.705	0.033	0.643	0.773	-
5	283	fixed effects	*gngt1*	0.099	0.098	-0.093	0.291	3.11E-01
			syt10	-0.056	0.065	-0.183	0.072	3.92E-01
			rgs6	-0.085	0.144	-0.366	0.197	5.55E-01
			hcn4	0.157	0.085	-0.010	0.325	6.54E-02
			hcn4l	0.198	0.158	-0.111	0.508	2.09E-01
			neo1a	0.007	0.086	-0.161	0.176	9.31E-01
			neo1b	-0.002	0.108	-0.213	0.210	9.86E-01
			kiaa1755_1	0.037	0.070	-0.100	0.175	5.94E-01
			kiaa1755_2	0.208	0.093	0.027	0.390	2.47E-02
			time of day	0.574	0.044	0.488	0.659	2.21E-39
			HRV (in SD)	-0.530	0.045	-0.617	-0.443	1.35E-32
			intercept	-2.187	0.377	-2.927	-1.448	6.58E-09
		random effects	variation by batch	0.617	0.204	0.323	1.178	-
			residual	0.684	0.029	0.629	0.743	-

Associations of heart rate variability (HRV) and heart rate (mutually adjusted) with the number of mutated alleles across the nine orthologues, weighted by their predicted effect on protein function. Associations were examined for the main transcript of each targeted zebrafish orthologue using hierarchical linear models (xtmixed in Stata), using inverse-normally transformed outcomes, so effect sizes and SEs can be interpreted as z-score units. Larvae with a sinoatrial pause before or after the recording were excluded from the analysis in this sensitivity analysis. Analyses were adjusted for time of day and the weighted number of mutated alleles in the other genes as fixed factors, with larvae nested in batches (random factor). For simplicity, *kiaa1755_1* refers to *quo*, and *kiaa1755_2* to *si:dkey-65j6.2*.

Supplementary Table 7: Transcript-specific association analyses for body size

		Body length									
		2dpf (n=332)					5dpf (n=240)				
Factor	**Gene**	**Effect size**	**SE**	**LCI**	**UCI**	**P**	**Effect size**	**SE**	**LCI**	**UCI**	**P**
fixed effects	*gngt1*	-0.053	0.114	-0.278	0.171	6.41E-01	0.027	0.112	-0.193	0.246	8.12E-01
	syt10	0.086	0.080	-0.070	0.242	2.79E-01	0.040	0.073	-0.103	0.183	5.85E-01
	rgs6	0.015	0.171	-0.321	0.350	9.31E-01	-0.271	0.157	-0.577	0.036	8.38E-02
	hcn4	-0.092	0.103	-0.294	0.109	3.69E-01	0.050	0.096	-0.138	0.238	6.02E-01
	hcn4l	0.159	0.204	-0.241	0.559	4.37E-01	-0.003	0.208	-0.411	0.406	9.90E-01
	neo1a	-0.201	0.103	-0.403	0.001	5.08E-02	0.061	0.094	-0.123	0.246	5.16E-01
	neo1b	-0.117	0.119	-0.350	0.116	3.26E-01	-0.079	0.118	-0.311	0.152	5.02E-01
	kiaa1755_1	0.107	0.078	-0.046	0.260	1.70E-01	-0.005	0.075	-0.152	0.143	9.50E-01
	kiaa1755_2	-0.208	0.107	-0.417	0.001	5.12E-02	-0.071	0.107	-0.281	0.139	5.07E-01
	Time of day	0.113	0.042	0.030	0.195	7.49E-03	0.081	0.048	-0.013	0.175	9.26E-02
	Intercept	0.166	0.330	-0.480	0.812	6.15E-01	-0.235	0.429	-1.077	0.607	5.84E-01
random effects	Variation by batch	0.407	0.131	0.217	0.764	-	0.711	0.231	0.376	1.345	-
	Residual	0.897	0.035	0.831	0.969	-	0.719	0.033	0.657	0.787	-

		Dorsal body surface area									
		2dpf (n=322)					5dpf (n=233)				
Factor	**Gene**	**Effect size**	**SE**	**LCI**	**UCI**	**P**	**Effect size**	**SE**	**LCI**	**UCI**	**P**
fixed effects	*gngt1*	0.112	0.109	-0.101	0.324	3.04E-01	-0.328	0.136	-0.595	-0.060	1.63E-02
	syt10	-0.057	0.076	-0.206	0.091	4.48E-01	-0.040	0.087	-0.211	0.132	6.48E-01
	rgs6	0.038	0.163	-0.282	0.358	8.16E-01	-0.135	0.191	-0.508	0.239	4.80E-01
	hcn4	-0.106	0.098	-0.298	0.086	2.80E-01	-0.016	0.113	-0.238	0.205	8.84E-01
	hcn4l	-0.151	0.196	-0.535	0.233	4.41E-01	0.359	0.243	-0.118	0.835	1.41E-01
	neo1a	0.218	0.099	0.025	0.412	2.66E-02	0.025	0.113	-0.195	0.246	8.23E-01
	neo1b	-0.100	0.115	-0.325	0.126	3.86E-01	-0.075	0.147	-0.363	0.213	6.12E-01
	kiaa1755_1	0.016	0.075	-0.131	0.163	8.32E-01	0.006	0.090	-0.170	0.183	9.43E-01
	kiaa1755_2	0.060	0.102	-0.139	0.259	5.55E-01	-0.015	0.127	-0.264	0.233	9.03E-01
	Time of day	-0.046	0.040	-0.125	0.032	2.49E-01	-0.084	0.055	-0.192	0.024	1.26E-01
	Intercept	-0.152	0.338	-0.815	0.510	6.52E-01	0.386	0.383	-0.365	1.137	3.13E-01
random effects	Variation by batch	0.492	0.154	0.267	0.910	-	0.325	0.127	0.151	0.697	-
	Residual	0.842	0.034	0.779	0.911	-	0.852	0.040	0.777	0.934	-

		Lateral body surface area									
		2dpf (n=300)					5dpf (n=256)				
Factor	**Gene**	**Effect size**	**SE**	**LCI**	**UCI**	**P**	**Effect size**	**SE**	**LCI**	**UCI**	**P**
fixed effects	*gngt1*	-0.056	0.121	-0.293	0.181	6.41E-01	-0.063	0.124	-0.306	0.179	6.09E-01
	syt10	0.042	0.085	-0.124	0.208	6.21E-01	0.027	0.083	-0.135	0.189	7.45E-01
	rgs6	-0.128	0.183	-0.487	0.231	4.84E-01	-0.022	0.175	-0.365	0.322	9.01E-01
	hcn4	0.151	0.108	-0.061	0.363	1.64E-01	-0.087	0.107	-0.297	0.122	4.14E-01
	hcn4l	-0.047	0.221	-0.479	0.385	8.32E-01	0.442	0.216	0.019	0.864	4.04E-02
	neo1a	-0.036	0.110	-0.252	0.180	7.42E-01	-0.024	0.107	-0.234	0.186	8.23E-01
	neo1b	0.257	0.130	0.002	0.512	4.80E-02	-0.096	0.141	-0.373	0.180	4.96E-01
	kiaa1755_1	0.027	0.085	-0.140	0.194	7.52E-01	0.099	0.088	-0.073	0.271	2.61E-01
	kiaa1755_2	-0.224	0.117	-0.454	0.005	5.53E-02	0.018	0.120	-0.216	0.252	8.79E-01
	Time of day	-0.049	0.045	-0.138	0.039	2.72E-01	-0.070	0.052	-0.173	0.032	1.79E-01
	Intercept	0.061	0.335	-0.595	0.718	8.55E-01	0.073	0.391	-0.694	0.839	8.53E-01
random effects	Variation by batch	0.340	0.117	0.173	0.669	-	0.471	0.162	0.240	0.924	-
	Residual	0.914	0.038	0.843	0.991	-	0.829	0.037	0.760	0.905	-

		Body volume									
		2dpf (n=299)					5dpf (n=198)				
Factor	**Gene**	**Effect size**	**SE**	**LCI**	**UCI**	**P**	**Effect size**	**SE**	**LCI**	**UCI**	**P**
fixed effects	*gngt1*	-0.051	0.111	-0.270	0.167	6.45E-01	-0.071	0.132	-0.330	0.187	5.88E-01
	syt10	0.008	0.079	-0.147	0.163	9.20E-01	0.046	0.082	-0.114	0.207	5.73E-01
	rgs6	-0.250	0.181	-0.606	0.106	1.68E-01	-0.202	0.173	-0.542	0.137	2.43E-01
	hcn4	0.123	0.099	-0.070	0.317	2.12E-01	-0.044	0.104	-0.249	0.160	6.71E-01
	hcn4l	-0.066	0.194	-0.446	0.314	7.35E-01	0.319	0.246	-0.163	0.800	1.94E-01
	neo1a	0.105	0.103	-0.097	0.307	3.07E-01	0.043	0.105	-0.162	0.248	6.82E-01
	neo1b	0.175	0.121	-0.063	0.413	1.49E-01	-0.061	0.146	-0.347	0.225	6.78E-01
	kiaa1755_1	-0.035	0.079	-0.190	0.120	6.57E-01	0.192	0.083	0.028	0.355	2.14E-02
	kiaa1755_2	-0.019	0.106	-0.226	0.188	8.58E-01	-0.036	0.124	-0.279	0.207	7.72E-01
	Time of day	-0.056	0.042	-0.139	0.027	1.85E-01	-0.053	0.053	-0.158	0.051	3.18E-01
	Intercept	-0.184	0.345	-0.860	0.492	5.94E-01	-0.296	0.441	-1.160	0.569	5.03E-01
random effects	Variation by batch	0.496	0.155	0.268	0.916	-	0.598	0.199	0.311	1.149	-
	Residual	0.841	0.035	0.776	0.912	-	0.733	0.037	0.663	0.809	-

Associations were analyzed for the main transcript of each targeted zebrafish orthologue using hierarchical linear models (xtmixed in Stata) using inverse-normally transformed outcomes, so effect sizes and SEs can be interpreted as z-score units. Associations were adjusted for time of day and for the weighted number of mutated alleles in the other genes as fixed factors, with larvae nested in batches (random factor). For simplicity, *kiaa1755_1* refers to *quo*, and *kiaa1755_2* to *si:dkey-65j6.2*.

Supplementary Table 8: Druggability of interacting partners

Candidate	Interaction partner	DGIdb categories	Drug available? (y/n)	Drug name (FDA approved)	Drug category
	GNAI1	Tumor supressor	y		
	GNAI3				
	GNAL				
	GNAS	Druggable genome, Drug resistance, Clinically actionable	y	Fluorouracil	Anti-neoplastic agents
	GNAT1				
	GNB1				
	GNB2	Transporter, Ion channel			
	GNB3				
	GNB4				
	GNB5	Transporter, Ion channel			
GNGT1	*OR10W1*	Druggable genome, G-protein coupled receptor			
	OR1L6	Druggable genome, G-protein coupled receptor			
	OR2AJ1	Druggable genome, G-protein coupled receptor			
	OR4C5	Druggable genome, G-protein coupled receptor			
	OR4F21	Druggable genome, G-protein coupled receptor			
	OR4K15	Druggable genome, G-protein coupled receptor			
	OR51H1	Druggable genome, G-protein coupled receptor			
	PDC	Phospolipase			
	PDCL				
	PLEKHB1				
	RHO	Druggable genome, G-protein coupled receptor	y	Halothane	Anestethics
				Telmisartan, Irbesartan, Valsartan, Eprosartan, Losartan	Anti-hypertensive agents
				Atorvastatin	Anti-cholesterimic agents
	AGTR1	Druggable genome, G-protein coupled receptor, Phospolipase	y	Cyclosporine	Immunosuppresive agents
				Indomethacin, Dexamethasone	Anti-inflammatory agents
				Levodopa	Anti-parkinson agents
	GNAI1	Tumor supressor	y		
	GNAI3				
	GNAT1				
	GNAT2	G-protein coupled receptor			
GNG11	*GNAT3*				
	GNB1				
	GNB2	Transporter, Ion channel			
	GNB3				
	GNB4				
	NMB	Druggable genome, Hormone activity			
	PDC	Phospolipase			
	PTGIR	Druggable genome, G-protein coupled receptor	y	Iloprost, Treprostinil, Selexipag, Epoprostenol	Anti-hypertensive agents
				Dinoprost thromethamine, Misoprostol	Abortifacient agents
	SMURF1				
	BOP1	Tumor supressor			
	SNAP23	Druggable genome			
	SNAP25	Druggable genome	y	Diazoxide	Anti-hypertensive agents
SYT10				Botulinum toxin type A	Neuromuscular blocking agents
	SNAP29	Druggable genome			
	SNAP47				
	SYT6				
	HCN1	Druggable genome, Transporter, Ion channel	y	Ivabradine	Channel blocker
HCN4	*HCN2*	Druggable genome, Transporter, Ion channel	y		
	HCN3	Druggable genome, Transporter, Ion channel	y	Ivabradine	Channel blocker
	PEX5L				
	CDH15				
	CDON				
	HFE2	Kinase, Serine-threonine kinase, Cell surface			
	NTN1	Druggable genome			
	NTN3	Druggable genome			
	NTN4	Druggable genome			
NEO1	*PITPNA*	Transporter			
	PTK2	Druggable genome, Kinase, Tyrosine kinase, Lipid kinase	y		
	RGMA				
	RGMB				
	TTN	Druggable genome, Kinase, Serine-threonine kinase, Tyrosine kinase			
	UNC5B				
KIAA1755	-				

Human candidate genes were examined for their interaction partners using STRING and Genemania, and their classification according to the Drug gene interaction database (DGIdb). Proteins that are already targeted by a drug are indicated by a "y". A selection of FDA-approved drugs was distilled from DGIdb, including their categorization.